A Semi-Analytical Model for Buckling of Stiffened Cylindrical Shells

by

Elisabeth Slettum

THESIS

for the degree of

Master of Science

(Master i Anvendt matematikk og mekanikk)

Faculty of Mathematics and Natural Sciences
University of Oslo

June 2013

Det matematisk- naturvitenskapelige fakultet
Universitetet i Oslo

Preface

The work outlined in this thesis has been carried out at the University of Oslo, Faculty of Mathematics and Natural Sciences, Department of Mathematics, from August 2012 to June 2013. I am grateful to my supervisor Associate Professor Lars Brubak at University of Oslo and Dr. Eivind Steen at Det Norske Veritas for great guidance and follow-up. I would like to thank the people at the Ship Structures and Concepts department at Det Norske Veritas for creating a welcoming and supportive environment. I would also like to thank my fellow students Preben Brekke Rotwitt, Mads Høgberget and Simen Kongshaug for academic discussions and moral support.

University of Oslo, 20. June 2013

Elisabeth Slettum

Summary

Cylindrical shells are common configurations within the technology. The transition from the side to the bottom on a ship has the shape of a fourth of a cylindrical shell. Both ring and stringer stiffeners can be added to the shell for support. Buckling of this type of structure is an important area of interest.

The main purpose of this thesis has been to make a semi-analytical model that can describe how a ring stiffened shell and stringer stiffened shell respond during buckling. A variety of loads have been subjected to the shell model. Simple analytical expressions do not exist for clamped shells or shells subjected to shear and numerical methods must be used. The development of the model has been done by use of linear buckling theory and an energy method, the Rayleigh Ritz method. The model has been programmed in Fortran. Eigenvalues and associated eigenmodes have been found.

The semi-analytical model has been verified against the finite element analysis software Abaqus. The results from the models were in good agreement with each other. The apply of the semi-analytical model on a bilge structure showed a deviation in the results. A small difference in the boundary conditions, with the element model being stiffer due to the edges being held straight, was causing the deviation. The difference in the results from the semi-analytical model and the element model was smaller for the ring stiffened shell than for the unstiffened shell and the stringer stiffened shell. The buckling load calculated by the semi-analytical model were on the conservative side compared with the element model.

Table of Contents

Preface **i**

Summary **iii**

Symbols **ix**

1 Introduction **1**
1.1 Background and motivation 1
1.2 Objective and scope 2
1.3 Presentation of chapters 3

2 General theory **5**
2.1 Introduction 5
2.2 Basic elasticity theory 5
2.3 Geometric nonlinearity 7
2.4 Theory of shells 8
2.5 Ring and longitudinal stiffeners 12
2.6 Buckling theory 12
2.7 Buckling modes 14
2.7.1 Global buckling 15
2.7.2 Local buckling 15
2.8 Imperfection sensitivity 17
2.9 Material properties 18

3 Relevant analysis methods **19**
3.1 Introduction 19
3.2 Eigenvalue problem 19
3.3 The Finite Element Method 20
3.4 The Rayleigh-Ritz Method 23
3.5 The FEA software Abaqus 24
3.5.1 The prosess 25

3.5.2 Iteration method . . . 25
3.5.3 Element type . . . 25
3.5.4 Mesh density . . . 26
3.5.5 Boundary conditions . . . 26
3.6 Fortran . . . 26

4 Semi-analytical model for eigenvalue calculations 28
4.1 Introduction . . . 28
4.2 Displacement function . . . 28
4.3 Potential energy . . . 30
4.3.1 Strain energy of a shell . . . 30
4.3.2 Potential energy due to external loads . . . 31
4.3.3 Potential energy due to lateral pressure . . . 32
4.3.4 Potential energy due to stiffeners . . . 32
4.3.5 Rotational springs at the boundaries . . . 33
4.4 Material stiffness matrix . . . 33
4.5 Geometric stiffness matrix . . . 34

5 Verification of shell model 36
5.1 Introduction . . . 36
5.2 Interaction between axial compression and lateral pressure . . . 36
5.3 Unstiffened shell . . . 39
5.4 Ring stiffened shell . . . 45
5.5 Stringer stiffened shell . . . 50

6 Apply of the shell model 54
6.1 Introduction . . . 54
6.2 Comparing with an element model . . . 54
6.3 Unstiffened shell . . . 56
6.4 Ring stiffened shell . . . 59
6.5 Stringer stiffened shell . . . 60

7 Summary and conclusion 62
7.1 Introduction . . . 62
7.2 Semi-analytical model . . . 63
7.3 Suggestions for further work . . . 64

Appendix 67

A Buckling of shells **67**
A.1 Differentiated series expressions 67
A.2 Airy's stress function 68
A.3 Shell membrane energy 71
A.4 Shell bending energy 71
A.5 Ring stiffener 72
A.6 Longitudinal stiffener 72
A.7 External energy 72
A.7.1 Potential energy due to axial stresses 72
A.7.2 Potential energy due to stresses in the ring direction . 73
A.7.3 Potential energy due to shear stresses 74
A.7.4 Potential energy due to external pressure 75
A.8 Rotational springs 75
A.8.1 Rotational spring at x=0 75
A.8.2 Rotational spring at x=L 76
A.8.3 Rotational spring at θ=0 76
A.8.4 Rotational spring at θ=π/2 77

B Part of the Fortran code **78**
B.1 Properties 78
B.2 Eigenvalue 79

List of symbols

A	-	area, mm^2
$\mathbf{B}$	-	strain-displacement matrix
C	-	extensional stiffness parameter
D	-	bending stiffness parameter
$\boldsymbol{D}$	-	global degrees of freedom
E	-	Young's modulus, N/mm^2
E_{ijkl}	-	material stiffness tensor
G	-	shear modulus, N/mm^2
$\mathbf{F}$	-	volume forces vector
I	-	moment of inertia, mm^4
I_{xx}, I_{yy}	-	moment of inertia about the x- and y axis, respectively, mm^4
$\mathbf{K}$	-	material stiffness matrix
K^G	-	geometric stiffness matrix
K^R	-	ring stiffness matrix
K^L	-	stringer stiffness matrix
L	-	length of shell, mm
$\mathbf{L}_i$	-	transformation matrix
$M_x, M_\theta, M_{x\theta}$	-	bending and twisting moments, Nmm/mm
N	-	number of elements
$N_x, N_\theta, N_{x\theta}$	-	normal and shearing forces, N/mm
$\mathbf{N}$	-	matrix of shape functions
Q_x, Q_θ	-	transverse shearing forces, N/mm
$\mathbf{R}$	-	global load vector
$\{R\}^{cr}$	-	critical load
$\{R\}^{ref}$	-	reference load
S	-	surface
$S_x, S_\theta, S_{x\theta}$	-	applied in-plane stresses
T	-	potential energy due to external loads
U	-	strain energy

U^m_{shell}, U^b_{shell}	-	membrane and bending strain energy
U^R	-	potential energy due to ring stiffener
U^L	-	potential energy due to stringer stiffener
U^S	-	potential energy due to rotational springs
V	-	volume
Z	-	Batdorf parameter

a	-	radius of cylinder, mm
a_{ij}, a_{kl}	-	amplitudes
$\mathbf{d}$	-	nodal displacement vector
f	-	stress function
$f_i(x)$, $g_i(\theta)$	-	shape functions
h_w	-	height of web, mm
$\boldsymbol{k}$	-	element stiffness matrix
k_a, k_p, k_t	-	stress parameters
$k_{x=0}$, $k_{x=L}$, $k_{\theta=0}$, $k_{\theta=\frac{\pi}{2}}$	-	spring constants
m	-	global degrees of freedom
p	-	pressure
$\boldsymbol{r}$	-	element load vector
t	-	shell thickness, mm
t_f	-	thickness of flange, mm
t_w	-	thickness of web, mm
u, v, w	-	displacement components
$\mathbf{u}$	-	displacement field
w_f	-	width of flange, mm
x, θ, z	-	shell coordinates

β_x, β_θ	-	rotations of shell element relative to the θ and x coordinate directions
$\delta_{j,q}$, $\delta_{i,p}$, $\delta_{q,s}$, $\delta_{r,p}$	-	Kronecker's delta
$\boldsymbol{\varepsilon}$	-	strain vector
$\varepsilon_x, \varepsilon_\theta, \gamma_{x\theta}$	-	membrane strains
$\varepsilon_{xs}, \varepsilon_{\theta r}$	-	strains for stiffeners
$\kappa_x, \kappa_\theta, \kappa_{x\theta}$	-	curvature changes and twist
λ	-	load factor
λ_i	-	eigenvalues
λ^{cr}	-	critical buckling value

ν	-	Poisson's ratio
Π	-	Potential energy
σ_x, σ_θ, $\tau_{x\theta}$	-	normal stresses and shear stress in a cylinder N/mm^2
σ_x^{cr}, p^{cr}, $\tau_{x\theta}^{cr}$	-	critical stresses, N/mm^2
σ_F	-	yield stress, N/mm^2
$\mathbf{\Phi}$	-	surface tractions
$\triangle u(\theta)$, $\triangle v(x)$	-	shortening of shell in longitudinal- and ring direction, respectively

Chapter 1

Introduction

1.1 Background and motivation

Thin shells have a large area of use because of their intrinsic properties. One great benefit is a shell's high strength to weight relation which makes it very suitable in designs where low weight is important and large loads have to be supported. Shell structures are the most often used structural components in nature and technology [1]. Cylinders are common shell configurations within the technology. Because of its curvature a shell can carry transverse loading in an optimal way by in-plane membrane forces, despite an often extreme slenderness [1]. The use of thin shells are popular among different fields within engineering; civil, mechanical, aeronautical, marine, structural and chemical engineering to name a few. The shell principle is used in many applications like pipes, cooling towers, containments and bilges, the rounded portion forming a transition between the bottom and the side of a ship's hull.

It is important to know the physics of shell buckling to produce reliable structures where thin shells are important components and also to avoid unexpected catastrophic failures. In the everyday language the word buckling may refer to a sudden, catastrophic collapse where very large deformations are involved. From an engineering point of view, buckling has taken place before the deformations are very large. To the unaided eye the structure actually might appear to be undeformed or only slightly deformed [2]. As pointed out, a shell structure can carry great loads because of its curvature, but it is also this typical shape of a shell in combination with different types of loads that makes a shell very sensitive to imperfections. The imperfection

sensitivity may lead to a large difference between the theoretical buckling load and the true buckling load of a loaded shell. The true buckling load for a cylindrical shell subjected to axial compression has in the most extreme cases been as low as 10 to 20 percent of the corresponding theoretical buckling load [3]. A shell is so sensitive to imperfections that a poor designed shell structure can react almost "chaotic" and this is strongly apparent when it comes to buckling. To be sure to find a theoretical buckling load that will correspond to the real buckling load, the principle features of the carrying mechanisms of shells must be understood.

1.2 Objective and scope

A bilge, the structural part connecting the bottom and the side of a ship, is normally subjected to various load types as axial compression, lateral pressure and shear loading, separately or in combinations. For the bilge to be able to carry more load, stiffeners in the longitudinal direction and the ring direction can be applied to the bilge. The stiffeners are to be placed between girders, which are structural members providing support to the stiffeners, as can be seen in Fig.1.1.

Finite element analysis (FEA) software are great tools to calculate the buckling load of different structures, but they also require great knowledge from the users about the fundamental theory. Det Norske Veritas (DNV) has developed a buckling assessment software package called PULS (Panel Ultimate Limit State), which is based on advanced mathematical models and implemented into easy and intuitive user interfaces, so that more people can calculate the buckling limit without having the same knowledge as is required for a FEA software user. PULS is being used in designing and building of ships and offshore structures. The buckling strength of stiffened thin plate elements can be calculated in PULS, but finding the buckling strength of stiffened thin shell elements is not yet possible. The main objective of this thesis is to make a semi-analytical model, based on energy methods, that can calculate the buckling strength of a longitudinally and ring stiffened thin shell The FEA software Abaqus will be used to verify the semi-analytical model.

The semi-analytical model will be based on the Rayleigh-Ritz method. Strain energy expressions for the two types of stiffeners, longitudinal stiffeners and ring stiffeners, is to be found and added to the expression for the shell strain

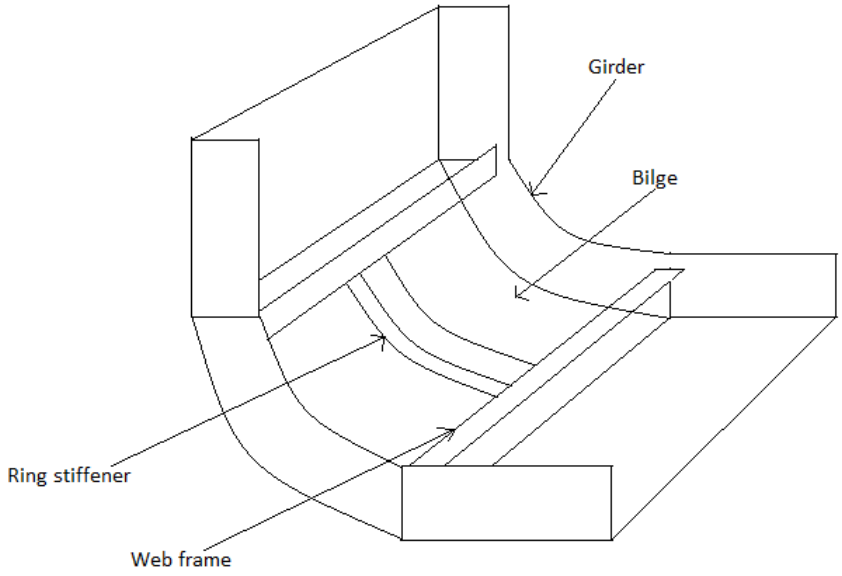

Figure 1.1: A ring stiffened bilge.

energy to provide greater support. The stiffeners are treated as discrete elements and the strain energy expression from each stiffener is added up to the equation. The second moment of inertia of a stiffener is freely chosen in the semi-analytical model and the buckling load and associated buckling mode of the shell is very much depending on this stiffener property.

The problem is limited to small deformations and linear elastic buckling theory is used. Steel and aluminum are both linear elastic materials used in structural applications and are suitable for use in the semi-analytical model.

1.3 Presentation of chapters

Chapter 2 is opening with an introduction of basic equations of elasticity. Shell theory and theory of buckling are presented next. Also an explanation of a shell's imperfection sensitivity can be found in this chapter.

In chapter 3 there will be a presentation of relevant methods used in this thesis to do a buckling analysis. An eigenvalue calculation and the finite element method is first presented. The semi-analytical model is based on an

energy method called the Rayleigh-Ritz, and its features are presented next. Displacement in the radial direction is assumed in the form of a trigonometric functions series. An overview of the FEA software Abaqus is also to be found in this chapter. An introduction to the imperative programming language Fortran is closing up the chapter.

In chapter 4 the semi-analytical model that has been made in this thesis is presented. The model represents a clamped cylindrical shell subjected to a variety of loading and it is including stiffeners in both the longitudinal direction and the ring direction.

In chapter 5 the semi-analytical model is verified against the FEA software Abaqus. The model is first verified for a clamped cylindrical shell without stiffeners and thereafter with ring stiffeners and finally with stiffeners in the longitudinal direction. The results are all presented graphically and a complementary discussion is following.

In chapter 6 the use of the semi-analytical model has been tried out. Buckling of a bilge, shaped as a fourth of a cylindrical shell, clamped in the ring direction and simply supported in the longitudinal direction and with stiffeners in between, is a typical case and how well this can be described by the model is tested in this chapter. Graphs are showing the results and a discussion is then following.

Conclusions on the work done in this thesis are found in chapter 7. Suggestion on further work is also to be found in this chapter.

Larger mathematical calculations have been put into the appendix to keep a greater overview of the results. Part of the Fortran code can also be found in the appendix.

Chapter 2

General theory

2.1 Introduction

When studying the theory of buckling of thin cylindrical shells, the understanding of the basic equations of elasticity and the concepts of work done and energy stored is needed. This chapter and the following chapter will give a general view of the topics mentioned above. Shell theory is presented in this chapter and general theory of buckling is introduced. In addition, different types of buckling modes of a stiffened shell will be looked into and imperfection sensitivity of a shell will be reviewed. Textbooks about general buckling theories have mainly been used for further reading [3, 4, 5, 6, 7, 8]. The equations in the further reading all apply for a linear elastic behavior under static load and response.

2.2 Basic elasticity theory

A material is said to be ideally elastic if the deformation of the material caused by a force is absolutely reversible when removing the same force, and at the same time there exists a linear and time independent relation between the state of stress and the state of strain. The theory of linear elasticity is based on several assumptions; small deformations, linear behavior of the material and dynamic effects being neglected. The material is also assumed to be homogeneous, i.e., its mechanical properties are the same at all points and isotropic, i.e., its mechanical properties are the same in all directions.

The generalized Hooke's law is describing the linear relationship between the state of stress and the state of strain. The relationship can be expressed mathematically as:

$$\sigma_{ij} = E_{ijkl}\varepsilon_{kl} \quad i,j,k,l = x,y,z \tag{2.2.1}$$

where the elements of the stiffness tensor E_{ijkl} are known as elastic coefficients. The first two subscripts of the stiffness tensor correspond to those of stress, whereas the last two subscripts correspond to those of strain. The elastic coefficients are assumed to be constant during deformation. Some quantities require a magnitude and two directions to fully describe them. Such quantities are called tensors of second-order. Stress and strain are both second-order tensors. The specification of stress requires both a force and a surface upon which the force acts.

In this thesis the elasticity limit is assumed to never be exceeded anywhere in the material, hence Hooke's law is always applicable. The stress and the strain in three dimensions can be written as vectors due to symmetry properties of σ_{ij} and ε_{kl}:

$$\boldsymbol{\sigma} = \begin{bmatrix}\sigma_x & \sigma_y & \sigma_z & \tau_{xy} & \tau_{yz} & \tau_{zx}\end{bmatrix}^T \tag{2.2.2}$$

$$\boldsymbol{\varepsilon} = \begin{bmatrix}\varepsilon_x & \varepsilon_y & \varepsilon_z & \gamma_{xy} & \gamma_{yz} & \gamma_{zx}\end{bmatrix}^T \tag{2.2.3}$$

where σ and ε are the normal stresses and normal strains and τ and γ are the shear stresses and shear strains, respectively. When applicable, only one subscript is used for simplicity.

The stress components for a thin shell are expressed in the cylindrical coordinates x and θ. See Fig.(2.1) for a representation of a shell's coordinate system. Distances from the middle surface of the cylindrical shell are measured by a coordinate z. When a shell is thin relative to the dimensions in the $x\theta$-plane a plane stress model can be used. For isotropy and plane stress conditions which are $\sigma_z = \tau_{\theta z} = \tau_{xz} = 0$, Hooke's law for thin shells can be written as:

$$\sigma_x = \frac{E}{1-\nu^2}(\varepsilon_{xx} + \nu\varepsilon_{\theta\theta}) \tag{2.2.4}$$

$$\sigma_\theta = \frac{E}{1-\nu^2}(\varepsilon_{\theta\theta} + \nu\varepsilon_{xx}) \tag{2.2.5}$$

$$\tau_{x\theta} = \frac{E}{2(1+\nu)}\gamma_{x\theta} = G\gamma_{x\theta} \tag{2.2.6}$$

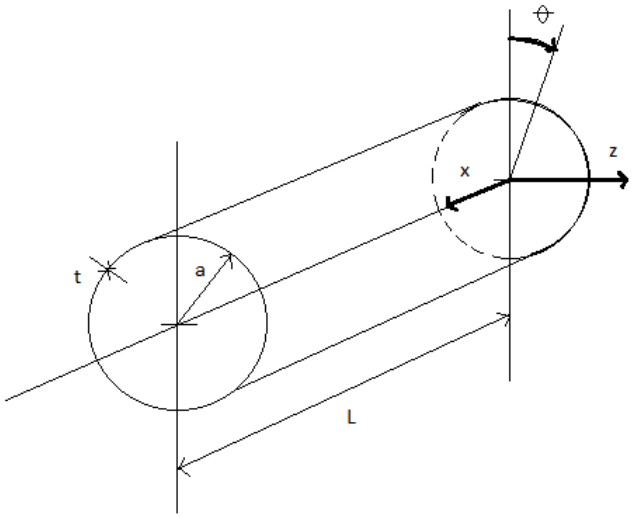

Figure 2.1: The shell's coordinate system.

where E is the elastic modulus, ν is the Poisson's ratio and G is the shear modulus. As can be seen in (2.2.6) the constant G is related to E and ν by the relation $G = E/2(1+\nu)$. The inverse relation of Hooke's law can be written as:

$$\varepsilon_{xx} = \frac{1}{E}(\sigma_{xx} - \nu\sigma_{\theta\theta}) \tag{2.2.7}$$

$$\varepsilon_{\theta\theta} = \frac{1}{E}(\nu\sigma_{xx} - \sigma_{\theta\theta}) \tag{2.2.8}$$

$$\gamma_{x\theta} = \frac{2(1+\nu)}{E}\tau_{x\theta} = \frac{1}{G}\tau_{x\theta} \tag{2.2.9}$$

2.3 Geometric nonlinearity

When a structure is subjected to a load it will deform and the geometry of the structure will change. As the structure deforms changes in stiffness and load direction will occur. If the deformations are small compared to the structure's characteristic size, these changes can be neglected and the equilibrium equations will be written with respect to the initial undeformed geometry. On the other hand, if the deformations are large, the geometric changes have to be taken into consideration, hence require that the structure should be in equilibrium when it is in a deformed shape. This means that the equilibrium equations are no longer linear with reference to the displacements

and geometric nonlinearity is therefor introduced. Large strains and large rotations are also examples of geometric nonlinearity. The effects described are often called second order effects.

As mentioned, the load direction will change as the structure deforms. In an analysis the change of direction can be accounted for in two ways; a following load or a non following load. A following load, also known as a nonconservative load, will change its direction when the structure upon which the load is working is deforming. It will also remain normal to the deformed structure. A non following load, known as a conservative load, retains its original direction after the structure deforms. Fig.2.2 shows an example of each of the two types. For the further work of this thesis a conservative load will be used.

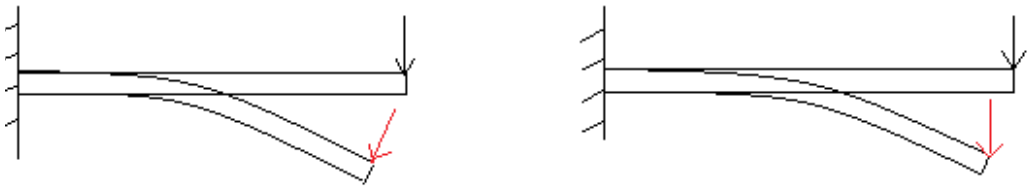

Figure 2.2: A nonconservative load to the left and a conservative load to the right.

2.4 Theory of shells

A shell can be defined as a body with curved inner and outer surfaces and where the distance between the two surfaces, the thickness t, is small compared to other dimensions of the body. The middle surface of the shell is at a distance $t/2$ from both surfaces. There are two types of shells: thin shells and thick shells. A shell is regarded as thin if the following condition is satisfied [9]:

$$max(\frac{t}{a}) \leq \frac{1}{20} \tag{2.4.1}$$

where a is the radius of curvature of the middle surface. As follows, the shell is thick if the inequality in (2.4.1) is not satisfied.

To describe a circular cylindrical shell a cylindrical coordinate system is applied to the cross-sectional area of the shell as shown in Fig.(2.1). The three axes are the longitudinal axis x, the circumferential axis θ and the transverse axis z. For a cylindrical shell the radius in the x-direction is infinite, hence its curvature is equal to zero. The radius in the θ-direction is equal to a constant a.

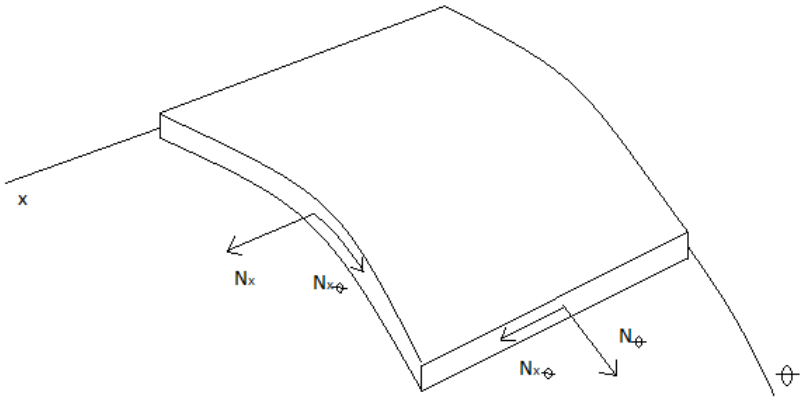

Figure 2.3: Cylindrical shell element.

The stress components of an elastic shell are linearly distributed across the shell thickness and it is then possible to express the internal forces and moments by integrating the stress distribution through the shell thickness:

$$\begin{aligned}
N_x &= \int_{-t/2}^{t/2} \sigma_x (1 + \frac{z}{a}) dz & N_\theta &= \int_{-t/2}^{t/2} \sigma_\theta dz \\
N_{x\theta} &= \int_{-t/2}^{h/2} \tau_{x\theta} (1 + \frac{z}{a}) dz & N_{\theta x} &= \int_{-t/2}^{t/2} \tau_{\theta x} dz \\
Q_x &= \int_{-t/2}^{t/2} \tau_{xz} (1 + \frac{z}{a}) dz & Q_\theta &= \int_{-t/2}^{t/2} \tau_{\theta x} dz \\
M_x &= r \int_{-t/2}^{t/2} \sigma_x (1 + \frac{z}{a}) z dz & M_\theta &= r \int_{-t/2}^{t/2} \sigma_\theta z dz \\
M_{x\theta} &= r \int_{-t/2}^{t/2} \tau_{x\theta} (1 + \frac{z}{a}) z dz & M_{\theta x} &= r \int_{-t/2}^{t/2} \tau_{\theta x} z dz
\end{aligned} \tag{2.4.2}$$

where $N_x, N_{x\theta}, N_\theta, N_{\theta x}$ are in-plane normal and shearing forces and Q_x, Q_θ are transverse shearing forces, both measured in N/mm. M_x, M_θ are bending moments and $M_{x\theta}, M_{\theta x}$ are twisting moments, both measured in Nmm/mm. The symbols $\sigma_x, \tau_{x\theta}$, etc. are stress components at any point through the shell thickness. For a thin shell the thickness to radius ratio z/r in relevant expressions in (2.4.2) can be neglected and hence $N_{\theta x} = N_{x\theta}$ and $M_{\theta x} = M_{x\theta}$. The transverse shearing forces are equal to zero since plane stress conditions are assumed for thin shells.

Expressions for the normal and shear strain components at an arbitrary point across the shell thickness include both the in-plane strain components at the middle surface and the changes in curvature and twist. The two types of strain are both given in terms of the middle surface displacements. The strain-displacement relationship can be written as:

$$\begin{aligned} \varepsilon_x^z &= \varepsilon_x - z\kappa_x \\ \varepsilon_\theta^z &= \varepsilon_\theta - z\kappa_\theta \\ \gamma_{x\theta}^z &= \gamma_{x\theta} - 2z\kappa_{x\theta} \end{aligned} \tag{2.4.3}$$

where z is the distance from the middle surface and $\varepsilon_x, ..., \kappa_{x\theta}$ represents the strain and curvature components of the middle surface. The kinematic relations for the middle surface of a shell is given by Donnel [3] as

$$\begin{aligned} \varepsilon_x &= u_{,x} + \frac{1}{2}\beta_x^2 & \beta_x &= -w_{,x} & \kappa_x &= \beta_{x,x} \\ \varepsilon_\theta &= \frac{v_{,\theta} + w}{a} + \frac{1}{2}\beta_\theta^2 & \beta_\theta &= -\frac{w_{,\theta}}{a} & \kappa_\theta &= \frac{\beta_{\theta,\theta}}{a} \\ \gamma_{x\theta} &= (\frac{u_{,\theta}}{a} + v_{,x}) + \beta_x\beta_y & & & \kappa_{x\theta} &= \frac{1}{2}(\frac{\beta_{x,\theta}}{a} + \beta_{\theta,x}) \end{aligned} \tag{2.4.4}$$

where a is the radius of the cylinder and u, v and w are the additional displacements induced by buckling. A comma denotes partial differentiation with respect to the subscript. The equations in (2.4.4) are valid for moderately large deflections. Additional terms are required in the strain and curvature relations for larger deflection.

In comparison to ε_y for plates the circumferential strain ε_θ in (2.4.4) has an extra term, w/a. This term arises from a larger circumference of the shell caused by a uniform radial expansion w. Before deformation the diameter of the shell is $2a$ and after deformation it is $2(a + w)$. The additional term to the circumferential strain is obtained in the following manner:

$$\overline{\varepsilon}_\theta = \frac{\triangle\text{circumference}}{\text{circumference}} = \frac{2\pi(a+w) - 2\pi a}{2\pi a} = \frac{w}{a} \tag{2.4.5}$$

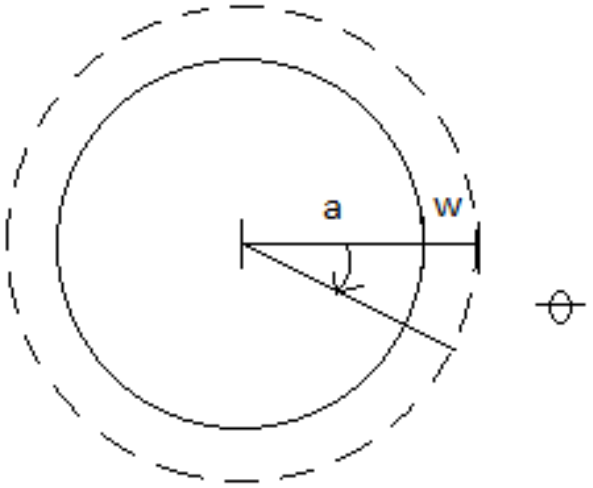

Figure 2.4: Radial expansion w of a shell subjected to a load.

The internal forces N_x, N_θ and $N_{x\theta}$ and moments M_x, M_θ and $M_{x\theta}$ can be expressed in terms of six quantities: the three components of strain ε_x, ε_θ and $\gamma_{x\theta}$ of the middle surface and the three curvature changes κ_x, κ_θ and $\kappa_{x\theta}$

$$\begin{aligned} N_x &= C(\varepsilon_x + \nu\varepsilon_\theta) \quad M_x &&= D(\kappa_x + \nu\kappa_\theta) \\ N_\theta &= C(\varepsilon_\theta + \nu\varepsilon_x) \quad M_\theta &&= D(\kappa_\theta + \nu\kappa_x) \\ N_{x\theta} &= C\frac{1-\nu}{2}\gamma_{x\theta} \quad M_{x\theta} &&= D(1-\nu)\kappa_{x\theta} \end{aligned} \tag{2.4.6}$$

where $C = \frac{Eh}{1-\nu^2}$ and $D = \frac{Eh^3}{12(1-\nu^2)}$. Eqs (2.4.6) are the constitutive equations for a thin-walled cylindrical shell.

By introducing a new function called the Airy stress function $f(x, \theta)$, the compatibility equation for a shell as shown by Donnel [3] can be written:

$$\bigtriangledown^4 f - \frac{E}{a^4}(w_{,x\theta}^2 - w_{,xx}\, w_{,\theta\theta} + a w_{,xx}) = 0 \tag{2.4.7}$$

where the following relations are true:

$$\sigma_x = f_{,\theta\theta} \quad \sigma_\theta = a^2 f_{,xx} \quad \tau_{x\theta} = -a f_{,x\theta} \tag{2.4.8}$$

Airy's stress function is only a function of the applied stresses and is not depending on the deformations. A solution to Eq. (2.4.7) is needed for calculation of a shell's membrane energy later in this thesis.

2.5 Ring and longitudinal stiffeners

We assume for the stiffeners to behave as beam elements. The strain-displacement relations for the stiffeners can then be written as

$$\begin{aligned} \varepsilon_{xs} &= \varepsilon_x - z\kappa_x \\ \varepsilon_{\theta r} &= \varepsilon_\theta - z\kappa_\theta \end{aligned} \tag{2.5.1}$$

where the subscripts s and r indicate stringers and rings, respectively.

During a deformation of a ring the normals to the undeformed centroidal surface are assumed to remain plane, normal and inextensional. The normal force N and the bending moment M on a ring cross section are defined as

$$N = \int \bar{\sigma} dA \quad \text{and} \quad M = \int \bar{\sigma} z dA \tag{2.5.2}$$

where $\bar{\sigma}$ is, as given by Hooke's law, $E\bar{\varepsilon}$, and is the normal stress in the θ direction of the ring. $\bar{\sigma}$ is also called the hoop stress and $\bar{\varepsilon}$ the hoop strain. Introducing the strain and curvature in Eq.(2.5.2), and integrating, gives

$$N = EA\varepsilon \quad \text{and} \quad M = EI\kappa \tag{2.5.3}$$

The equations in (2.5.3) are the constitutive relations for a ring. For the ring stiffener the curvature is given as:

$$\kappa_\theta = \frac{1}{a^2}(w - w_{,\theta\theta}) \tag{2.5.4}$$

For the longitudinal stiffener the curvature is given as:

$$\kappa_x = w_{,xx} \tag{2.5.5}$$

Only the bending part of the stiffeners will be used in the semi-analytical model since this part is much larger than the extension part.

2.6 Buckling theory

What distinguish shells from plates is the additional characteristic of curvature. A shell's behavior under an applied force is primarily governed by the curvature. Shells are, due to the curvature, more complicated than flat

plates because their bending cannot be separated from their stretching.

The membrane stiffness of a shell is in general several orders of magnitude greater than the bending stiffness. A thin shell can absorb a great amount of membrane strain energy without deforming too much. However, if the shell is loaded in such a way that most of the strain energy is in the form of membrane compression, and at the same time there is a way that this energy can be converted to bending energy, the shell may buckle. The exchange from membrane energy to bending energy causes the shell to buckle. To convert a given amount of membrane energy into bending energy large deflections are generally required. The way in which buckling occurs depends on how the shell is loaded and material properties of the structure.

The critical load is defined as the smallest load at which the equilibrium of the structure fails to be stable as the load is slowly increased from zero [3]. With bifurcation buckling this critical point may be defined as an equilibrium state where two equilibrium paths intersect. Bifurcation buckling can be divided into two categories; Asymmetric and symmetric bifurcation. The two types can further be categorized as stable, hence not sensitive of imperfections or unstable and then imperfection sensitive. Equilibrium is always stable below the bifurcation point and unstable above it for the primary path. An additional study of the secondary path must be performed to be able to decide whether or not the bifurcation point is in stable equilibrium. If the initial part of the secondary path has a positive slope, as is the case for a flat plate, the bifurcation point is stable. The bifurcation point is unstable if the secondary path has a negative slope, as is the case for a shell.

Snap-through-buckling occurs when the shell has reached a limit point. A dynamic process is then taking place until a new stable equilibrium configuration is gained. Perfect shells under certain load conditions and shells with imperfection patterns typically experience this type of buckling. The critical load is obtained through solution of nonlinear equations of equilibrium.

A shell under identical loading and boundary conditions may have several possible equilibrium configurations. In some cases the buckling load at a bifurcation point is not necessarily equal to the maximum load the structure can support. In other cases the predicted bifurcation buckling load of the structure can never be reached in experiments.

There is a fundamental difference in the behavior of plates and shells exposed to compression stresses. For the plate, an additional strength is achieved after

buckling and a greater load than the critical load might be acceptable. The postcritical strength is due to membrane forces arising as the load increases. Membrane behavior becomes more significant as deflections increase. For a thin-walled cylinder the maximum load is much less than the theoretical critical load. This is because of a high sensitivity to geometric imperfections.

2.7 Buckling modes

When a stiffened shell is exposed to a minimum critical load it will buckle into a certain mode. Properties that influence the buckling mode are, among others, the load type, type of stiffener; ring stiffeners, longitudinal stiffeners or a combination of the two, and the bending stiffness of both the shell and the shell stiffeners. The different types of buckling modes of a stiffened shell can further be divided into two main groups; global buckling modes and local buckling modes.

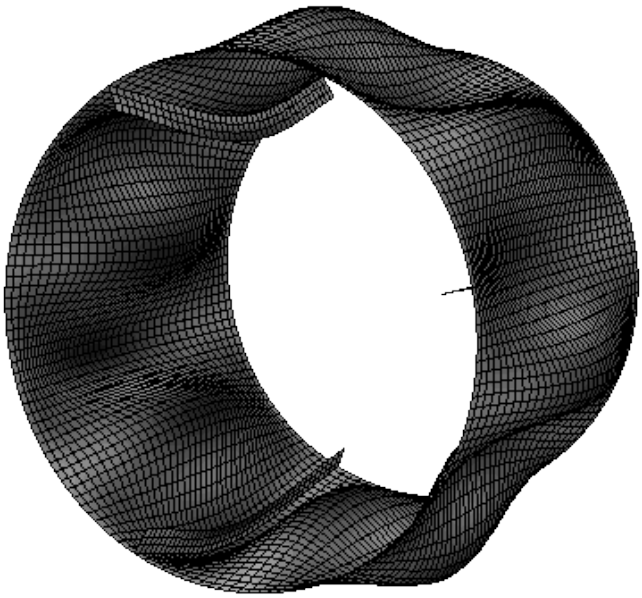

Figure 2.5: Global buckling of a stringer stiffened cylindrical shell.

2.7.1 Global buckling

General buckling of a structure including a shell and its stiffeners is the case where the bending stiffness of the stiffeners do not contribute considerably to prevent a displacement of the shell in the z-direction and the stiffeners then buckle in the same manner as the shell. The buckling mode is as if the stiffeners were not represented and the shell is then carrying most of the load. An example of a global buckling mode for a shell with longitudinal stiffeners exposed to lateral pressure has been modeled in Abaqus and is shown in Fig.(2.5). As can be seen, the three longitudinal stiffeners are following the buckling mode of the shell and the buckling mode is global.

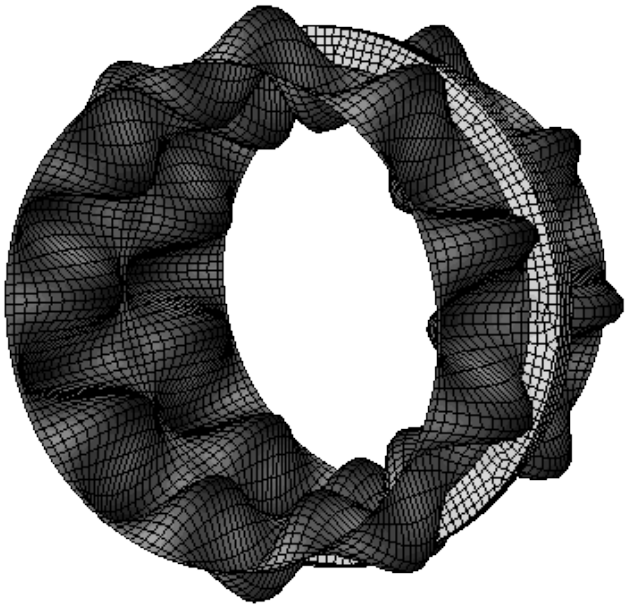

Figure 2.6: Local shell buckling of a ring stiffened cylindrical shell.

2.7.2 Local buckling

The biggest contribution to the bending stiffness of different stiffeners is the second moment of inertia. The magnitude of the second moment of inertia is depending on the shape and the dimensions of the shell stiffener. If the stiffener's bending stiffness is to that extent that it will not buckle when the shell is exposed to a critical load that is making the shell itself buckle, the buckling mode is local to the shell only. Shell buckling is one example

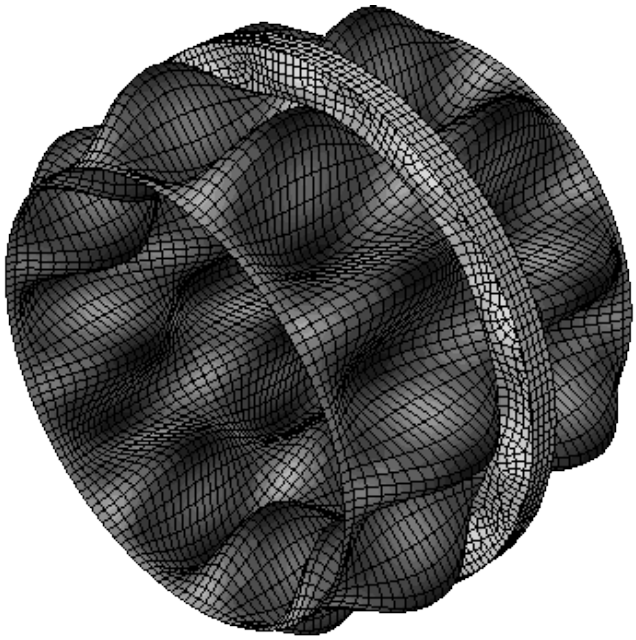

Figure 2.7: Local shell buckling and buckling of a stiffeners web for a ring stiffened cylindrical shell.

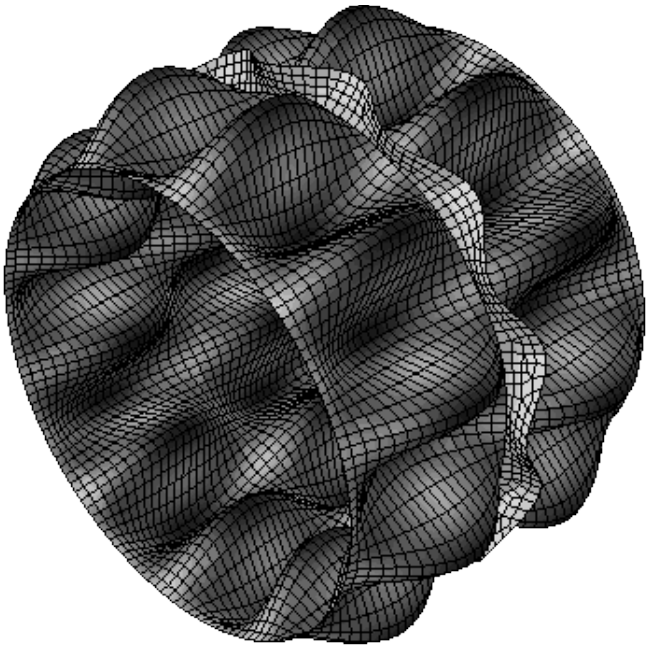

Figure 2.8: Local shell buckling and torsional buckling of stiffener for a ring stiffened cylindrical shell.

of a local buckling mode and it is demonstrated in Fig.(2.6). The shell in this figure is stiffened by a ring stiffener placed at $L/2$ and it buckles into a half wavelength on each side of the stiffener in the longitudinal direction. Long half waves in the longitudinal direction is an expected buckling mode for a shell subjected to lateral pressure. Local buckling can arise in both the shell and the web of the stiffener as seen in Fig.(2.7). When the torsional stiffness of the stiffener is small it rotates about its own axis as can be seen in Fig.(2.8).

2.8 Imperfection sensitivity

As with the case of the buckling phenomenon in a structure and a model being different due to imperfections as described in section 2.6, the magnitude of the buckling load is also influenced by imperfections. The term imperfection sensitivity is expressed by Bushnell [10] as: "The sensitivity of the load at which a shell buckles to imperfections in the shape of the shell".

The degree of sensitivity of a shell can be divided into three categories; highly, moderately and not imperfection-sensitive. This depends on the nature of the structure and the loading. A cylindrical shell under axial compression is highly imperfection-sensitive. This is because the critical buckling load corresponds to a mode where the axial and the circumferential wavelengths are quite small compared to the radius. Axially compressed stiffened cylindrical shells, externally pressurized cylindrical shells and cylindrical shells under uniform torsion can be put into the mid category. The characteristic of this category is that the wavelength of the buckles are of the same order as a typical overall dimension of the shell, e.g. the length of the shell. Also the buckling eigenvalues corresponding to different modes of buckling do not gather as densely as is the case with highly imperfection sensitive shells.

The source of a shells imperfection sensitivity is the interaction of many various buckling modes having the same or nearly the same critical load. This interaction at the beginning of the postcritical response also causes the buckling mode to change at larger deflections. For an imperfection-sensitive structure the first eigenmode may not characterize the deformation that leads to the lowest buckling load.

An initial imperfection is a small accidental deviation from the assumed initial shape of a structure. The shell geometry and its boundary conditions

have imperfections affecting the initial deformation when a shell structure is loaded. Residual stresses can also contribute to imperfections in the shell, but the imperfections are mainly due to the first two.

Because of imperfections in a structure there can be a significant difference between the theoretical buckling load calculated and what is the actual buckling load, and for some cases a nonlinear analysis has to be performed to predict a buckling load as close to the actual buckling load as possible. When doing a nonlinear analysis, the first step is to define the shape of an initial imperfection. For a flat plate it is normal to use the buckling mode associated with the smallest eigenvalue from a linear analysis as the imperfection because this is normally the same as the critical collapse mode. The shell geometry is more complicated and doing the same for a shell as with a plate will not necessarily give the lowest buckling load. This is because, for shells, as described earlier, there is an interaction of various buckling modes occurring at the same load. The shell structure may snap over to a more preferred shape than the imperfection shape and this leads to an unstable response. A shape requiring less internal strain energy is preferred. The tendency is to use a combination of several buckling modes from the linear buckling analysis. The combination of modes that gives the lowest buckling load is to be used. The amplitude of the imperfection should be small because more energy is required to change the buckling mode with a large magnitude and the structure may then be forced into a non-preferred shape [13]. A linearized analysis will in many cases give suitable results for design use. In this thesis, only linear buckling analyses have been performed.

2.9 Material properties

The material in the analyses in this thesis, for both the cylindrical shell and the ring- and longitudinal stiffeners, is steel and its properties are:

Property	**Value**
Young's modulus, E $[N/mm^2]$	206000
Poisson ratio, ν	0.3

Steel is an isotropic material, hence its properties are equal in every direction.

Chapter 3

Relevant analysis methods

3.1 Introduction

The Rayleigh-Ritz method and the Finite Element Method (FEM) are two examples of numerical solution methods. When problems that have to do with buckling of cylindrical shells are to be solved, analytical methods can't always be used because of the complexity of the problems and numerical methods are then selected as solution methods. The background information for this chapter is obtained from [5, 6, 11].

3.2 Eigenvalue problem

A linear eigenvalue analysis predicts the theoretical buckling strength of an ideal elastic structure. The initial imperfections in the structure are assumed to be neglected and the analysis is therefore limited to symmetric bifurcation. For a shell, who exhibits an unstable symmetric buckling behavior when a critical load is being reached, the calculated strength can be a serious overestimate.

Membrane stresses, who act tangent to the midsurface of a shell and arising from axial loading, has an influence on the lateral deflection of the shell. These internal stresses cause second order strain stiffening, also called geometric stiffening, which are significant compared with the elastic bending stiffness and must therefore be included in the total stiffness of the struc-

ture. A geometric stiffness matrix K_G accounts for the effects of membrane stresses on lateral deflection in the total stiffness. The geometric stiffness K_G is a function of the stress, which is directly proportional to the loading. The geometric stiffness matrix is also independent of material properties.

When a structure is loaded with a reference level of external load $\{R\}^{ref}$, the geometric stiffness matrix is $\left[K_G(\sigma)\right]^{ref}$ for the associated stresses. For some other load level the geometric stiffness matrix can be written in terms of the reference geometric stiffness matrix and a scalar multiplier λ:

$$\left[K_G(\sigma)\right] = \lambda \left[K_G(\sigma)\right]^{ref} \quad \text{when} \quad \{R\} = \lambda\{R\}^{ref} \tag{3.2.1}$$

λ is called a load factor. The equilibrium equation for the structure is written as:

$$(\left[K\right] - \lambda \left[K_G(\sigma)\right]^{ref})\{D\} = \lambda\{R\}^{ref} \tag{3.2.2}$$

where $[K]$ is the material stiffness matrix and $[K_G(\sigma)]^{ref}$ is the geometric stiffness matrix. $\{D\}$ is the displacement vector and $\{R\}^{ref}$ is the load vector due to external loads. External loads do not change at at a bifurcation point and the equilibrium equation is then written as:

$$(\left[K\right] - \lambda_i \left[K_G(\sigma)\right]^{ref})\{\delta D\} = \{0\} \tag{3.2.3}$$

where $\{\delta D\}$ is a small increment in displacement and λ_i are eigenvalues. The structure buckles when the load factor is equal to the lowest eigenvalue. The lowest eigenvalue is hence being the critical value. The critical load can then be written as:

$$\{R\}^{cr} = \lambda^{cr}\{R\}^{ref} \tag{3.2.4}$$

Every eigenvalue has an associated eigenvector. The eigenvector represents the buckling shape characteristic for the corresponding critical buckling value. The eigenvector only gives the shape of the deformation and not the size. It is useful to also know the higher values of λ since this will provide information of how separated the buckling loads are. Postbuckling mode jumps are more likely to happen when the buckling loads are dense.

3.3 The Finite Element Method

The finite element method (FEM) is a numerical approach to approximately solve partial differential equations describing physical phenomena in engineering. The idea of FEM is to divide a body into finite elements. This

division simplifies the task of generating approximation functions. Also, the devision allows for a representation of the solution over individual elements. In this way, geometric and material discontinuities can naturally be included. The elements are connected to neighboring elements at global nodes. The particular arrangement of elements is called a mesh. The smaller the mesh the more accurate the result will be. Loads and boundary conditions are applied at the nodes. Since the elements are connected to each other at the nodes, the solutions from various elements connected at a node must have the same value at that node.

FEM is based on assuming a displacement field $\mathbf{u}$. The displacement field is always based on polynomials. The displacement field can be written in terms of shape functions:

$$\mathbf{u} = \mathbf{N}\mathbf{d} \tag{3.3.1}$$

where $\mathbf{u}$ is the displacement field, $\mathbf{N}$ is a matrix of shape functions and $\mathbf{d}$ is the nodal displacement vector of an element. The shape functions depend on the type of element and the number of nodes. The strain-displacement relation can be expressed as:

$$\boldsymbol{\varepsilon} = \boldsymbol{\partial}\mathbf{u} \tag{3.3.2}$$

where $\boldsymbol{\varepsilon}$ is the strain vector and $\boldsymbol{\partial}$ is a partial derivative matrix. If $\mathbf{u}$ is substituted into (3.3.2), the strains can be expressed in terms of the element shape functions and the nodal displacements:

$$\boldsymbol{\varepsilon} = \boldsymbol{\partial}\mathbf{N}\mathbf{d} = \mathbf{B}\mathbf{d} \tag{3.3.3}$$

where $\mathbf{B}$ is a strain-displacement matrix. Only the shape functions have to be differentiated in order to find the strains since the nodal displacement vector does not depend on x, y or z.

The potential energy Π is a function of a function, known as a functional. The total potential energy Π in a body is given as the difference between the strain energy stored in the element and the work done on the element [6]:

$$\Pi = \frac{1}{2}\int_V \boldsymbol{\varepsilon}^T\boldsymbol{\sigma}dV - \int_V \mathbf{u}^T\mathbf{F}dV - \int_S \mathbf{u}^T\boldsymbol{\Phi}dS \tag{3.3.4}$$

where $\mathbf{F}$ are volume forces and $\boldsymbol{\Phi}$ are surface tractions. Using Hooke's law and substituting the strain expression from (3.3.2) into the total potential energy expression gives:

$$\Pi = \frac{1}{2}\int_V \mathbf{d}^T\mathbf{B}^T\mathbf{E}\mathbf{B}\mathbf{d}dV - \int_V \mathbf{d}^T\mathbf{N}^T\mathbf{F}dV - \int_S \mathbf{d}^T\mathbf{N}^T\boldsymbol{\Phi}dS \tag{3.3.5}$$

Using the principle of stationary potential energy [6] on Eq.(3.3.5), where the variation operation is related to the undetermined coefficients $\mathbf{d}$, and taking advantage of the fact that the strain energy density is a scalar function, thus equal to its own inverse, gives the following result:

$$\delta\Pi = \delta\mathbf{d}^T(\int_V \mathbf{B}^T\mathbf{E}\mathbf{B}dV\mathbf{d} - \int_V \mathbf{N}^T\mathbf{F}dV - \int_S \mathbf{N}^T\mathbf{\Phi}dS) = 0 \tag{3.3.6}$$

The condition in Eq.(3.3.6) has to be satisfied for any arbitrary choice of $\delta\mathbf{d}^T$, hence the content in the paraenthesis can be set to zero. From (3.3.6) we find the element stiffness matrix and the load vector to be:

$$\boldsymbol{k} = \int_V \mathbf{B}^T\mathbf{E}\mathbf{B}dV\ , \quad \boldsymbol{r} = \int_V \mathbf{N}^T\mathbf{F}dV + \int_S \mathbf{N}^T\mathbf{\Phi}dS \tag{3.3.7}$$

The element stiffness matrix $\boldsymbol{k}$ relate the displacements $\boldsymbol{d}$ to the forces $\boldsymbol{r}$ at the element nodes. A column of $\boldsymbol{k}$ is the vector of loads that must be applied to an element at its nodes to maintain a deformation state in which the corresponding nodal degrees of freedom has unit value while all other nodal degrees of freedom are zero [6].

The nodal displacements for every element are subsets of the global displacements and the relation between them is given as:

$$\boldsymbol{d}_i = \boldsymbol{L}_i\boldsymbol{D} \tag{3.3.8}$$

where $\boldsymbol{L}_i$ is a $m_i \times m$ transformation matrix. m_i is the number of degrees of freedom in element i and m is the total number of global degrees of freedom. $\boldsymbol{L}_i$ contains ones where local degrees of freedom and global degrees of freedom are related and zeros for the rest of the matrix. For a larger structure containing many elements, the transformation matrix for every element is very sparse.

Both $\boldsymbol{k}$ and $\boldsymbol{r}$ are augmented so that they can be summed to a global stiffness matrix and a global load vector, respectively. Summation of the element stiffness matrices and the element load vectors gives:

$$\boldsymbol{K} = \sum_{i=1}^{N} \boldsymbol{L}_i^T\boldsymbol{k}_i\boldsymbol{L}_i\ , \quad \boldsymbol{R} = \sum_{i=1}^{N} \boldsymbol{L}_i^T\boldsymbol{r}_i \tag{3.3.9}$$

where $\boldsymbol{K}$ is a $m \times m$ matrix, $\boldsymbol{R}$ is a $m \times 1$ vector and N is the number of elements. An assembly of element stiffness matrices make up the global

stiffness matrix which relates the displacements of the nodes of the mesh to applied external forces:

$$\mathbf{KD} = \mathbf{R} \tag{3.3.10}$$

By solving this equilibrium equation, the displacements of the structure are found.

In a computer software, $\boldsymbol{K}$ is at first a null matrix and $\boldsymbol{R}$ is at first a null vector, the stiffness coefficients and the nodal loads of each element is then, in turn, added directly to appropriate locations in the global matrix $\boldsymbol{K}$ and $\boldsymbol{R}$. This is called the direct stiffness method.

Strain and stress fields may display greater error than the displacement field. To obtain the strain-displacement matrix [**B**] the displacement field has to be differentiated as seen in Eq.(3.3.3). Differentiation discloses differences and therefor give rise to the greater error appearing in the strain and stress fields in comparison with the displacement field.

3.4 The Rayleigh-Ritz Method

Partial differential equations describe the behavior of a continuum, such as an elastic solid. Given that a continuum consists of an infinite number of degrees of freedom (DOF's), each of them describing the displacements of a particle of the material, it will be impossible to find a displacement field that solves the differential equations and satisfies the boundary conditions. Instead of searching for the exact deformation shape, approximate deformation functions as a set of linear independent shape functions in combination with undetermined parameters to describe the deformation is used. The problem is then reduced from one of infinitely many DOF's to one with a limited number of DOF's.

The Rayleigh-Ritz method begins with approximating fields for displacement components to obtain a solution to a given problem. For a thin shell, which is a two dimensional problem, the radial deflection can be described by:

$$w = \sum_{ij}^{mn} a_{ij} f_i(x) g_j(\theta) \tag{3.4.1}$$

where a_{ij} are amplitudes and f_i and g_j are shape functions. The shape functions must be linear independent and also satisfy compatibility conditions

and essential boundary conditions. Displacements and rotations at the edges are a shell's essential boundary conditions. Functions satisfying the requirements stated above are called admissible functions. For a shell the natural boundary conditions are the forces and moments at the edges. The shape functions do not have to satisfy the natural boundary conditions, but a better result is to be expected if also the force conditions are satisfied.

To determine the DOF's, Eq.(3.4.1) is substituted into the expressions for normal and shear strains in the total potential energy functional Π. The functional is now a function of the parameters $a_{11}, a_{21}, ..., a_{mn}$. Since this has to be satisfied for arbitrary variations, all the partial derivatives have to be equal to zero. In a simplified manner this can be written as

$$\frac{\partial \Pi}{\partial a_{ij}} = 0 \quad for \quad i, j = 1, 2, ..., m, n \tag{3.4.2}$$

This is a system of $m \times n$ algebraic equations with $m \times n$ unknowns. The simultaneous solution of these equations makes up a matrix eigenvalue problem and by solving this system of equations the unknown parameters and the approximate solution for the displacement is found. Strains and stresses can be computed from the approximate displacement solution, but then generally less accurate than the displacements.

The Rayleigh-Ritz method will inevitably overestimate the buckling load, hence the answer calculated will always be on the insecure side. The structure is not allowed to conform to the buckling mode that fits it the best. Instead, the structure is forced to follow the chosen shape functions. As a consequence the calculated system if stiffer than the real one and the calculated buckling load becomes higher than what is to be expected. The inaccurateness of the buckling load depends on how well chosen the shape functions are to represent the real buckling mode. Additional DOF's included in the displacement functions will give a more accurate result, hence the error in the approximation will be reduced and the assumed solution converges to the exact solution from above.

3.5 The FEA software Abaqus

In this thesis a semi-analytical model has been created. To make sure that this model is providing a correct result it has been verified against a FEA software. Different software exist and for this thesis Abaqus has been chosen.

3.5.1 The prosess

A FEA consists of three steps; the pre-process, the process and the post-process. In the first step, the pre-process, the model is built and assigned properties, it is further divided into small elements and finally meshed. The second step is an evaluation and simulation of the model. An output visual file is produced in this step. In the third and final step, the results from the analysis is presented. The output file is used to generate a report, an image, an animation e.l. of the output that has been requested by user in an earlier step.

3.5.2 Iteration method

In the processing step of the buckling analysis a subspace iteration method is used. This method is computationally efficient when only a small number of eigenvalues p is sought. A selected matrix X of dimension $(n \times q)$, where n is degrees of freedom and $q = min(2p, p + 8)$ is the number of vectors used per iteration, defines a subspace. An iteration procedure is used, $K\overline{X}_{i+1} = K^G X_i$, to map the material stiffness matrix K and the geometric stiffness matrix K^G onto this subspace using $K_{i+1} = \overline{X}_{i+1}^T K \overline{X}_{i+1}$ and $K_{i+1}^G = \overline{X}_{i+1}^T K^G \overline{X}_{i+1}$. The iterations are continued until the required eigenvalues have been obtained.

3.5.3 Element type

To model the cylindrical shell in Abaqus, shell elements have been used. Such elements are used when the dimension of the thickness is significantly smaller than the other dimensions, and the shell structure is then being discretized by defining the geometry at a reference surface, the middle surface. The shell elements have six degrees of freedom at every node, three displacement degrees of freedom and three rotational degrees of freedom. In Abaqus there are general-purpose shell elements and shell elements that are valid for thin and thick shell problems. In this thesis $S4R$ shell elements have been used for the cylindrical shell. This general-purpose shell element becomes a discrete Kirchhoff thin shell element as the thickness decreases [12]. The transverse shear deformation becomes very small as the shell thickness decreases.

3.5.4 Mesh density

To be sure that the results in Abaqus have converged, smaller and smaller mesh refinements have been tried out. Analyses with mesh sizes as 50×50, 40×40 and 30×30 have been carried out. The run time of an analysis is significantly longer when a smaller mesh is used, so the biggest mesh that gives accurate buckling loads and a right description of the associated buckling modes is sought. For a cylindrical shell the buckling mode associated with the lowest eigenvalue is depending on the loading of the shell. A cylindrical shell subjected to an axial compressive load buckles into many halfwaves in both the longitudinal direction and in the ring direction and for the finite element program to pick up this buckling mode a very fine mesh size has to be used. For a cylinder subjected to lateral pressure and torsion a coarser mesh can be used and the buckling mode will be well presented. In conclusion, the mesh density chosen generally depends on geometrical proportions, load combinations and type of element. Four node shell elements have been used to model the cylindrical shell and also to model the web and flange of the stiffeners as described in [13].

3.5.5 Boundary conditions

The cylindrical shell is clamped at both ends. It is free to move in the longitudinal direction at one end and in the radial direction at both ends. An equation-function is applied to the ends, where the terms consist of a coefficient applied to a degree of freedom of every node in a set, and hence constraining the end nodes to move at an equal distance in the longitudinal direction when being subjected to a load. The stiffeners have no boundary conditions at its edges.

3.6 Fortran

For this thesis Fortran has been used as the programming tool. To be able to calculate the eigenvalue of the shell being analyzed a tool like this is of big necessity. The material stiffness matrix and the geometric stiffness matrix have been calculated analytically. The expressions have then been implemented into Fortran where the lowest eigenvalue is calculated.

Clamped boundary conditions are counted for by rotational springs. The magnitude of the spring stiffeners can be set to any value and a high stiffness can in that way model a rigid supported shell by preventing rotation at the boundaries. Both the strain energy part from the longitudinal stiffeners and the strain energy part from the ring stiffeners make a contribution to the material stiffness matrix.

Chapter 4

Semi-analytical model for eigenvalue calculations

4.1 Introduction

In this chapter the strain energy for the parts contributing to the total potential energy expression for the semi-analytical model will be presented. A material stiffness matrix and a geometric stiffness matrix has been found. The model is implemented into Fortran to find the eigenvalues. Background material for this chapter is found in [3, 14, 15].

4.2 Displacement function

The lateral displacement of a cylindrical shell subjected to different types of loads can be described by a sum of displacement functions in a Rayleigh-Ritz model. The following sum of displacement functions has been chosen to describe the deformation of both an unstiffened clamped cylindrical shell and a stiffened clamped cylindrical shell subjected to a load:

$$w = \sum\sum a_{ij} \sin\left(\frac{\pi i}{L}x\right) \sin\left(2j\theta\right) \quad \begin{matrix} 0 \leq x \leq L \\ 0 \leq \theta \leq \dfrac{\pi}{2} \end{matrix} \tag{4.2.1}$$

where a_{ij} are amplitudes, L is the length of the shell and θ is the angle in the circumferential direction. The better the displacement functions can de-

scribe the buckling mode of the shell, the more exact the result will be. The function in Eq.(4.2.1) is a sum of multiple sine functions. The cylindrical shell is being clamped at both ends and the rotation at both ends is thereby equal to zero. Every single term itself in (4.2.1) can not describe a clamped end, but as a sum, zero rotation at each end is very well described. Only odd terms are needed due to symmetry in the boundary conditions.

The displacement function also has to satisfy no lateral displacement at both ends. Because of Poisson's transverse contraction relation the shell will expand in the radial direction when it is subjected to axial compression. This is a static displacement and it is not making a contribution to the principle of stationary energy. The displacement functions are therefor only describing the buckling mode.

Both the ring stiffener and the longitudinal stiffener are assumed to follow the displacement of the shell when the shell is subjected to a load and the same displacement function is used in the stiffeners' strain energy expressions.

The shell model can be subjected to axial compression, lateral pressure and shear loading. When the shell is subjected to lateral pressure circumferential stress must be applied to maintain equilibrium. The relationship between the two can be written as:

$$S_\theta = \frac{a}{t}p \tag{4.2.2}$$

The intention is to find a scalar λ^{cr} so that the critical stress is equal to the applied stress multiplied by λ^{cr}. For the different types of loads mentioned above the following is to be found:

$$\sigma_x^{cr} = \lambda^{cr} S_x \tag{4.2.3}$$

$$p^{cr} = \lambda^{cr} p \ = \lambda^{cr} \frac{t}{a} S_\theta \tag{4.2.4}$$

$$\tau_{x\theta}^{cr} = \lambda^{cr} S_{x\theta} \tag{4.2.5}$$

where S_x, p and $S_{x\theta}$ are reference stresses.

4.3 Potential energy

Each volume element of a body possesses a potential energy which depends on a local state of deformation. In an elastic structure, work done by internal forces is equal in magnitude to the change in strain energy. The external forces are those transmitted by the body and these forces can be divided into two groups; volume forces and surface forces. The minus sign facing the potential energy of external forces indicates that the work is applied on the body as opposed to work stored in the body.

4.3.1 Strain energy of a shell

The strain energy of an isotropic shell, without initial stresses $\boldsymbol{\sigma}_0$ and initial strains $\boldsymbol{\varepsilon}_0$, is given in terms of stresses and strains:

$$U_{shell} = \int_V \frac{1}{2}\boldsymbol{\sigma}^T\boldsymbol{\varepsilon} dV = \int_V \frac{1}{2}\boldsymbol{\varepsilon}^T\mathbf{E}\boldsymbol{\varepsilon} dV \tag{4.3.1}$$

For a simply supported shell without stiffeners the energy in (4.3.1) is the strain energy needed to deform the shell over its volume. The strain energy of a shell can be divided into two parts; membrane strain energy and bending strain energy. The membrane energy can be expressed as:

$$U^m_{shell} = \frac{aC}{2}\int_0^{\frac{\pi}{2}}\int_0^L \left[(\varepsilon^m_x + \varepsilon^m_\theta)^2 - 2(1-\nu)(\varepsilon^m_x\varepsilon^m_\theta - (\varepsilon^m_{x\theta})^2)\right] dxd\theta \tag{4.3.2}$$

To calculate the membrane strain energy, Airy's stress function $f(x,\theta)$ has been used. An outline of the calculation can be seen in the appendix. For the bending strain energy the calculation is more straight forward. Inserting the middle-surface moment-curvature relations from (2.4.6) into (4.3.1), the potential energy can be written in terms of the displacement function:

$$U^b_{shell} = \frac{aD}{2}\int_0^{\frac{\pi}{2}}\int_0^L \left[\left(w_{,xx} + \frac{w_{,\theta\theta}}{a^2}\right)^2 - 2(1-\nu)\left(w_{,xx}\,\frac{w_{,\theta\theta}}{a^2} - \frac{w^2_{,x\theta}}{a^2}\right)\right] dxd\theta \tag{4.3.3}$$

A more extensive calculation is to be found in the appendix. Both the membrane strain energy and the bending strain energy make a contribution to the total potential energy expression, hence:

$$U_{shell} = U^m_{shell} + U^b_{shell} \tag{4.3.4}$$

4.3.2 Potential energy due to external loads

When a conservative load is doing work on a structure, the structure is loosing potential. The lost potential due to external loads on the structure can in general be written as:

$$T = -\int_S \mathbf{u}^T \mathbf{\Phi} dS \tag{4.3.5}$$

where $\mathbf{\Phi}$ represents surface tractions, which are forces per unit of surface area, $\mathbf{u}$ represents displacements and S is the surface area. The negative sign in front of the integral is because the displacement is in the opposite direction of the positive coordinate direction. An axially compressive load is doing work on the body through the displacement it is causing and this work can be written as:

$$T_{S_x} = -\int_0^{\frac{\pi}{2}} tS_x \triangle u(\theta) a d\theta \tag{4.3.6}$$

where t is the thickness of the shell, S_x is the axial compressive load and $\triangle u(\theta)$ is the shortening of the shell in the longitudinal direction. $\triangle u(\theta)$ can be calculated as:

$$\triangle u(\theta) = \int_0^L u,_x^m \, dx = \int_0^L (\varepsilon_x^m - \frac{1}{2} w,_x^2) dx \tag{4.3.7}$$

where the expression in the last integral is taken from the middle-surface kinematic relations in (2.4.4). Lateral pressure is another type of load. For the body to be in static equilibrium when being exposed to lateral pressure, there has to be a force in the circumferential direction of the shell, S_θ. The strain energy for the circumferential load is:

$$T_{S_\theta} = -\int_0^L tS_\theta \triangle v(x) dx \tag{4.3.8}$$

where $\triangle v(x)$ is the displacement in the ring direction and can be calculated as:

$$\triangle v(x) = \int_0^{\frac{1}{2}} \frac{v,_\theta}{a} a d\theta = \int_0^{\frac{\pi}{2}} \left(\varepsilon_\theta - \frac{w}{a} - \frac{1}{2} \frac{w,_\theta{}^2}{a^2} \right) a d\theta \tag{4.3.9}$$

The strain energy of a shear load is written as:

$$T_{S_{x\theta}} = -\int_0^L \int_0^{\frac{\pi}{2}} tS_{x\theta} \left(\frac{u,_\theta}{a} + v,_x \right) a d\theta dx \tag{4.3.10}$$

$$= -\int_0^L \int_0^{\frac{\pi}{2}} tS_{x\theta} \left(\gamma_{x\theta} - w,_x \frac{w,_\theta}{a} \right) a d\theta dx \tag{4.3.11}$$

The contribution from the loads to the total potential energy expression can then be written as follows:

$$T = T_{S_x} + T_{S_\theta} + T_{S_{x\theta}} \tag{4.3.12}$$

Only constant loads are subjected to the shell in this thesis.

4.3.3 Potential energy due to lateral pressure

The strain energy because of lateral pressure is:

$$T_P = -\int_0^L \int_0^{\frac{\pi}{2}} pwd\theta dx \tag{4.3.13}$$

As shown in the appendix, (4.3.13) does not make a contribution in the principle of stationary potential energy because it does not contain a term a_{ij} of second order.

4.3.4 Potential energy due to stiffeners

A stiffened shell will be able to carry a heavier load than an unstiffened shell. To what extend depends on the load working and the type of stiffener being used. The strain energy of a stiffener gives a contribution in the semi-analytical model. For a ring stiffener the strain energy is given as:

$$U^R = \frac{2EI}{a^3} \int_0^{\frac{\pi}{2}} (w - w_{,\theta\theta})^2 d\theta \tag{4.3.14}$$

where E is the Young modulus of the ring stiffener and I is the second moment of inertia of the ring about the shells middle surface. Given that $r \approx a$, where r is the middle surface radius of the ring, the same radius as the shell can be used in (4.3.14). Eq.(4.3.14) is the strain energy of one ring, and by the use of more than one, the strain energy per ring has to be added. A shell can also be stiffened in the longitudinal direction and the strain energy of a longitudinal stiffener is given as:

$$U^L = \frac{EI}{2} \int_0^L w_{,xx}^2 \, dx \tag{4.3.15}$$

where E is the Young modulus of the longitudinal stiffener and I is the second moment of inertia of the stiffener about the shells middle surface. As with the ring, the strain energy of every longitudinal stiffener has to be added in the total potential energy expression.

4.3.5 Rotational springs at the boundaries

A clamped shell can be modeled with elastic springs to prevent rotation at the boundaries. The strain energy associated with the boundary at $x = 0$ can be written as:

$$U^S_{x=0} = \int_0^{\frac{\pi}{2}} \frac{1}{2} k_{x=0} w_{,x}^{\,2} \,|_{x=0} a d\theta \tag{4.3.16}$$

where $k_{x=0}$ is a spring constant and is given as the rotational stiffness of the spring at the boundary where $x = 0$. For the three other edges the strain energy expressions are similar and are written as:

$$U^S_{x=L} = \int_0^{\frac{\pi}{2}} \frac{1}{2} k_{x=L} w_{,x}^{\,2} \,|_{x=L} a d\theta \tag{4.3.17}$$

$$U^S_{\theta=0} = \int_0^{L} \frac{1}{2} k_{\theta=0} w_{,\theta}^{\,2} \,|_{\theta=0} dx \tag{4.3.18}$$

$$U^S_{\theta=\frac{\pi}{2}} = \int_0^{L} \frac{1}{2} k_{\theta=\frac{\pi}{2}} w_{,\theta}^{\,2} \,|_{\theta=\frac{\pi}{2}} dx \tag{4.3.19}$$

and again, the k's are the stiffnesses at the boundaries where they are represented. To make sure that there will be no rotation at the boundary, hence the shell having clamped edges, the rotational spring constants have to be very high. In the model of this thesis the constants are set to the highest possible values that the programming software can maintain.

4.4 Material stiffness matrix

The material stiffness matrix for a shell, which depends on material properties, can in general be calculates as:

$$K^M = \frac{\partial^2 U}{\partial a_{ij} \partial a_{kl}} \tag{4.4.1}$$

where U is the strain energy and a_{ij} and a_{kl} are amplitudes. The chain rule is used to compute the partial derivative to the first amplitude and the partial derivative to the second amplitude is then straight forward. Only strain energy expressions containing a_{ij} to the second power will make a contribution to the stiffness matrix. For the membrane and bending energy

of the shell, the following expressions occur:

$$\frac{\partial^2 U^m_{shell}}{\partial a_{ij}\partial_{kl}} = \frac{\pi LtEa}{8}\frac{\left(\frac{\pi i}{L}\right)^4}{\left(\left(\frac{\pi i}{L}\right)^2+\left(\frac{2j}{a}\right)^2\right)^2} \tag{4.4.2}$$

$$\frac{\partial^2 U^b_{shell}}{\partial a_{ij}\partial_{kl}} = \frac{\pi LDa}{8}\left(\left(\frac{\pi i}{L}\right)^2+\left(\frac{2j}{a}\right)^2\right)^2 \tag{4.4.3}$$

The stiffness of the ring and longitudinal stiffeners and the stiffness of the springs at the boundaries are calculated in the same manner as the material stiffness of the shell and in an eigenvalue problem the stiffener's and spring's stiffness are added to the shell's material stiffness:

$$((K^M + K^R + K^L + K^S) + \lambda K^G)D = 0 \tag{4.4.4}$$

For the stiffeners in the ring- and longitudinal directions the stiffness per stiffer is calculated as:

$$\frac{\partial^2 U^R}{\partial a_{ij}\partial_{kl}} = \frac{EI_{0r}\pi}{a^3}\left(1-(2j)^2\right)^2 \sin\left(\frac{\pi i}{L}\right)\sin\left(\frac{\pi p}{L}\right)\delta_{j,q} \tag{4.4.5}$$

$$\frac{\partial^2 U^L}{\partial a_{ij}\partial_{kl}} = \frac{EI_{0l}\pi^4}{4L^3} i^4 \sin(2j\theta)\sin(2q\theta)\delta_{i,p} \tag{4.4.6}$$

Rotational springs make the body stiffer and the stiffness at the various boundaries of the shell are calculated as:

$$\frac{\partial^2 U^S_{x=0}}{\partial a_{ij}\partial_{kl}} = \frac{a\pi^3 k_{x=0}}{4L^2} ik\delta_{q,s} \tag{4.4.7}$$

$$\frac{\partial^2 U^S_{x=L}}{\partial a_{ij}\partial_{kl}} = \frac{a\pi^3 k_{x=L}}{4L^2} jl\cos(\pi i)\cos(\pi k)\delta_{q,s} \tag{4.4.8}$$

$$\frac{\partial^2 U^S_{\theta=0}}{\partial a_{ij}\partial_{kl}} = 2k_{\theta=0} Lqs\delta_{r,p} \tag{4.4.9}$$

$$\frac{\partial^2 U^S_{\theta=\frac{\pi}{2}}}{\partial a_{ij}\partial_{kl}} = 2k_{\theta=\frac{\pi}{2}} Lqs\cos(\pi j)\cos(\pi l)\delta_{r,p} \tag{4.4.10}$$

4.5 Geometric stiffness matrix

For a shell the geometric stiffness matrix is accounting for the effects of the membrane stresses, which are acting tangent to the midsurface, on

lateral deflections. The geometric stiffness matrix is a function of the shell's geometry, displacement field and state of membrane stress, and it is, in opposite of the material stiffness, independent of material properties. It can in general be calculated as:

$$K^G = \frac{\partial^2 T}{\partial a_{ij} \partial a_{kl}} \tag{4.5.1}$$

A stress condition is causing a change in a body's geometry and this change is included in the geometric stiffness matrix. The contribution to the geometric stiffness matrix from an axial compressive load is:

$$\frac{\partial^2 T_{S_x}}{\partial a_{ij} \partial_{kl}} = -\frac{S_x t a L \pi}{8} \left(\frac{\pi i}{L}\right)^2 \tag{4.5.2}$$

The contribution from the stress in the circumferential direction due to lateral pressure:

$$\frac{\partial^2 T_{S_\theta}}{\partial a_{ij} \partial_{kl}} = -\frac{S_\theta t L \pi}{8a} (2j)^2 = -\frac{pL\pi}{8} (2j)^2 \tag{4.5.3}$$

When the shell is loaded with axial compression and lateral pressure, the material stiffness matrix must be supplemented by a pressure stiffness matrix to provide the correct buckling load.

The contribution to the geometric stiffness matrix because of a shear load is:

$$\frac{\partial^2 T_{S_{x\theta}}}{\partial a_{ij} \partial_{kl}} = -\frac{S_{x\theta} t i l}{4} I_{ijkl} \tag{4.5.4}$$

where

$$I_{ijkl} = \begin{cases} 0 & \text{if i=k or j=l} \\ \left(\frac{\cos((l-j)\pi)-1}{l-j} - \frac{\cos((l+j)\pi)-1}{l+j}\right) * & \\ \left(\frac{\cos((k-i)\pi)-1}{k-i} - \frac{\cos((k+i)\pi)-1}{k+i}\right) & \text{else} \end{cases} \tag{4.5.5}$$

Chapter 5

Verification of shell model

5.1 Introduction

In this chapter the results from the semi-analytical model are presented. For a clamped shell or a shell subjected to a shear load, an analytical solution can not be obtained and a FEA software like Abaqus is then a useful tool for comparison of results. In the semi-analytical model, Donnel's kinematic relations and Airy's stress function, both valid for a cylindrical shell, are used. A parameter study of how lateral pressure as a prestress is interacting with axial compression is presented. The semi-analytical model has been carried out on unstiffened cylindrical shells subjected to axial compression, uniform lateral pressure and shear loading. The same types of loads have then been applied to a ring stiffened shell and a stringer stiffened shell. The results from the semi-analytical model are compared to results from Abaqus for verification.

5.2 Interaction between axial compression and lateral pressure

The cylindrical shell studied in this thesis has been modeled as a full cylinder in Abaqus since Donnel's kinematic relations and Airy's stress function used in the semi-analytical model are valid for a complete cylindrical shell. The cylindrical shell is being clamped at its edges and in the semi-analytical

model this is taken into account by rotational springs, hence they may not rotate about the θ-axis. The edges are allowed to move in the radial direction in a cylindrical coordinate system since the radius is changing as an effect of the Poisson's transverse contraction relation when the shell is subjected to a load. One edge is also allowed to move in the longitudinal direction when load is subjected to the cylindrical shell.

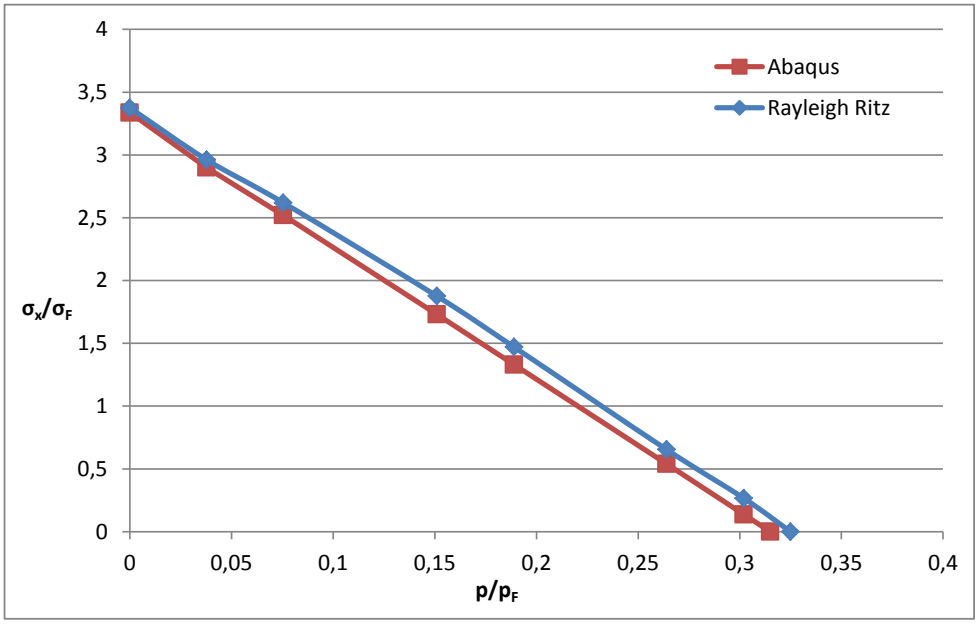

Figure 5.1: Interaction curves for a shell where $L = 3400mm$, $a = 1900mm$ and $t = 16mm$.

In the semi-analytical model, based on the Rayleigh-Ritz method, a finite number of terms in the sum has been used. As was described in chapter 4 the clamped edges could be described by the sum because each terms was canceling each other out leading towards zero rotation at the edge. Each term in the sum correspond to a degree of freedom. For the semi-analytical model a number of 30 degrees of freedom in the x-direction and 30 degrees of freedom in the θ-direction, with a total of 900 degrees of freedom, has been used. More degrees of freedom are included to make sure that the answer in converging toward the correct solution. For comparison, the number of elements for the shell studied in Fig.(5.1) in the element model is equal to 16320.

To see how axial compression and lateral pressure interact on the unstiffened clamped cylindrical shell, where the lateral pressure is applied as a

prestress and with an increase in value, an interaction curve has been made. The curve can be see Fig.(5.1). The relation between the pressure load and a given proportion of the yield stress represent the x-axis and the relation between the axial buckling load and the yield stress represent the y-axis. The yield stress of steel is given as:

$$\sigma_F = 315\text{MPa} \tag{5.2.1}$$

The size of p_F is here defined as a proportion of the yield stress where the magnitude is dependent on the thickness t and the radius a of the shell:

$$p_F = \frac{t}{a}\sigma_F \tag{5.2.2}$$

The dimensions of the cylindrical shell that is being studied in Fig.(5.1) are as follows:

L=3400mm a=1900mm t=16mm

From the graph in Fig(5.1) it can be seen that there is a linear coherence between the axial compression and the lateral pressure. When the lateral pressure is equal to zero, the axial force is the only force acting on the cylindrical shell and short half waves in both the longitudinal direction and the ring direction are dominating, as is to be expected from a shell subjected to axial compression. Buckling under a combination of axial compression and lateral pressure can be quite sensitive to imperfections, especially in cases where axial compression is dominating.

When lateral pressure is added as a prestress it has an impact on the buckling load and the associated buckling mode. The buckling mode is going from short half waves in both directions to only one halfwave in the longitudinal direction and 12 half waves in the ring direction for a complete cylinder. The latter is also the buckling mode of the shell loaded with lateral pressure only.

For a cylinder with a short length L and a thick thickness t, and in addition having clamped boundary conditions, the magnitude of the lateral pressure has to be larger than for a cylinder with a greater length and a smaller thickness to make the same interaction with the axial compressive load.

5.3 Unstiffened shell

Initially a model without stiffeners has been studied. In the next section a ring stiffener has been added to the model and the model is then verified against Abaqus and finally, longitudinal stiffeners are added to the model and verified against Abaqus.

The buckling load for every load case for various dimensions of the unstiffened cylindrical shell is calculated by the semi-analytical model and by an element model in Abaqus. The comparison of the results obtained in the semi-analytical model and the results obtained in Abaqus are shown graphically. In that matter it has been useful to introduce some nondimensional parameters for the x- and y-axes. The x-axis is represented by the Batdorf parameter Z:

$$Z = \frac{L^2}{at}\sqrt{1-\nu^2} \tag{5.3.1}$$

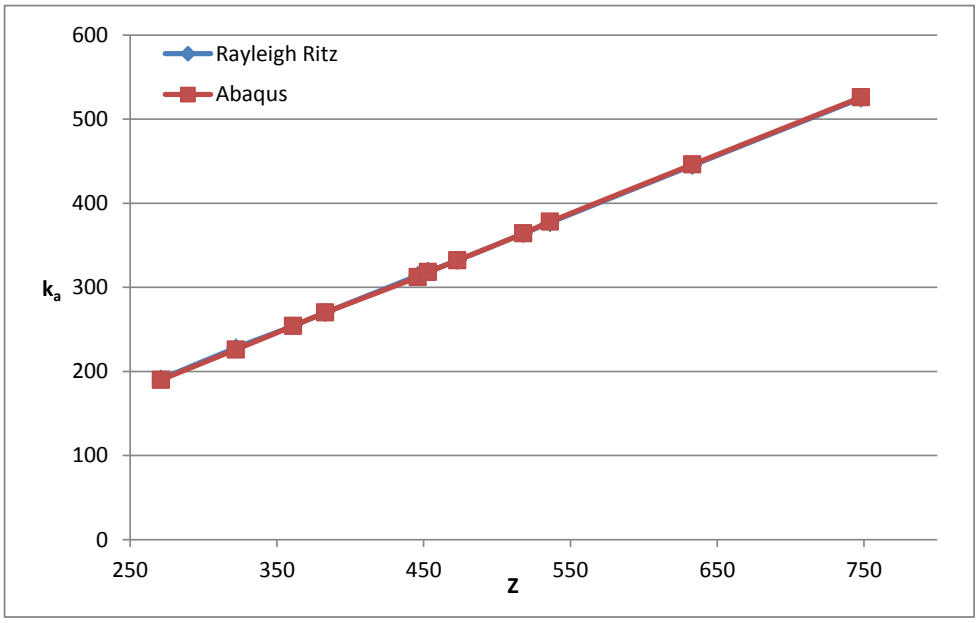

Figure 5.2: Critical values of axial stress for unstiffened cylindrical shells subjected to axial compression.

The Batdorf parameter is a cylinder geometry variable. L is the length of the cylinder, a is the radius, t is the thickness and ν is the Poisson ratio. The length of the cylinder studied in this thesis is varying from $3200mm$ to $4400mm$ and the thickness is varying from $13mm$ to $19mm$. The radius of the cylinder is kept constant at $1900mm$. The various dimensions are typical dimensions of a bilge on a ship.

For a cylindrical shell subjected to axial compression the following nondimensional parameter is introduced for the y-axis, representing the state of stress in the shell:

$$k_a = \frac{L^2 t}{\pi^2 D}\sigma_x^{cr} \tag{5.3.2}$$

where σ_{cr} is the critical stress defined in (4.2.3) and D is the bending stiffness. In Fig.(5.2) the results are shown graphically. Under the action of the axial compressive load, the cylinder shortens and the radius is increasing. The radius is also increasing at the ends, hence the ends in the model are allowed to move in the radial direction as mentioned.

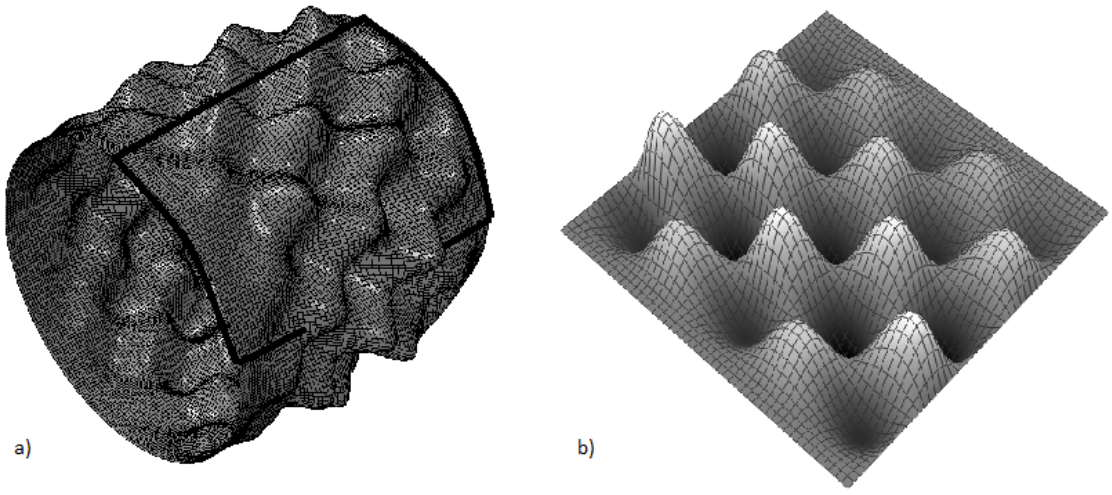

Figure 5.3: The buckling mode in a) Abaqus and b) Rayleigh Ritz of a cylindrical shell with L=4000mm, a=1900mm and t=15mm subjected to axial compression.

From the graph it can be seen that the model is very well describing a clamped cylindrical shell subjected to axial compression as the two graphs coincide. The coherence between Z and k_a is an almost straight line, and as

Z is increasing, the parameter k_a is also increasing. Fig.(5.3) is showing how a cylindrical shell subjected to axial compression buckles. The wavelengths in both the longitudinal direction and the ring direction are short with a number of five in both directions. Because an axially loaded shell buckles into many half waves in the longitudinal and the ring direction, the clamped boundary condition does not have a much greater effect on the buckling load compared to a simply supported shell.

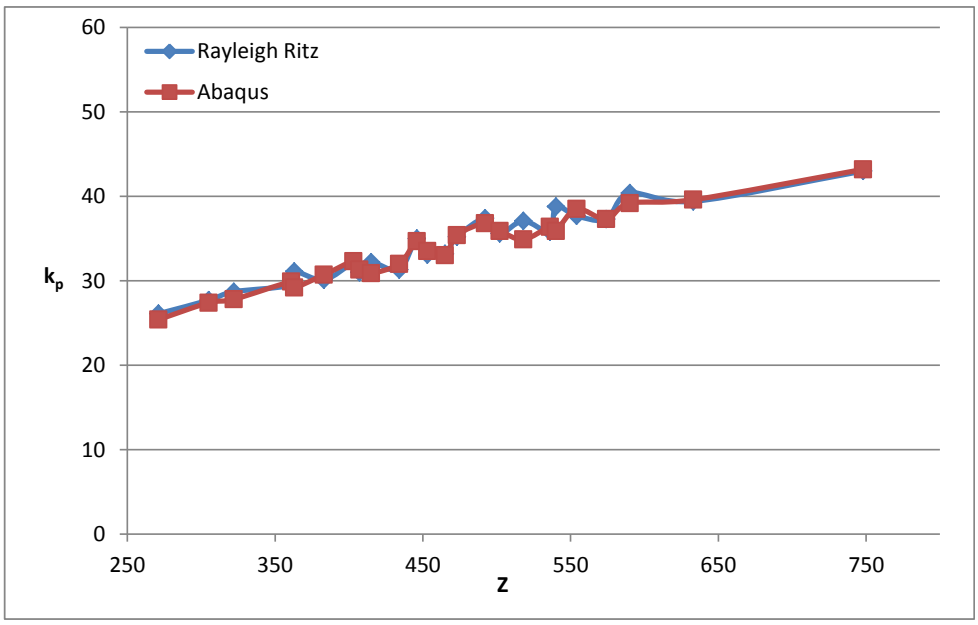

Figure 5.4: Critical values of pressure for unstiffened cylindrical shells subjected to lateral pressure.

Lateral pressure causes buckling by introducing a circumferential stress σ_θ. The circumferential stress, called the hoop stress, is related to the applied pressure p for a shell subjected to external lateral pressure. From equilibrium the relationship can be written as:

$$\sigma_\theta = \frac{a}{t}p \tag{5.3.3}$$

For the cylindrical shell subjected to lateral pressure the nondimensional parameter for the y-axis is:

$$k_p = \frac{L^2 a}{\pi^2 D}\sigma_\theta^{cr} \tag{5.3.4}$$

where σ_θ^{cr} is the critical load defined in (4.2.4) and a is the radius which is kept constant through the analyses. Since the cylindrical shell is free to extend in the longitudinal direction as the lateral pressure is applied the stress in this direction is equal to zero.

Fig.(5.4) is showing the results of critical values of pressure for unstiffened cylindrical shells subjected to lateral pressure. Unlike the almost straight line occurring for the axial loaded shells, the curve in Fig.(5.4) is moving up and down as Z is increasing. This is because the buckling load is changing as the buckling mode is changing with an increasing Z. For an axially loaded shell the higher order eigenvalues are very dense and close to the lowest eigenvalue and a change in the buckling mode along the x-axis will not make the buckling load change in the same manner as with the shell subjected to lateral pressure.

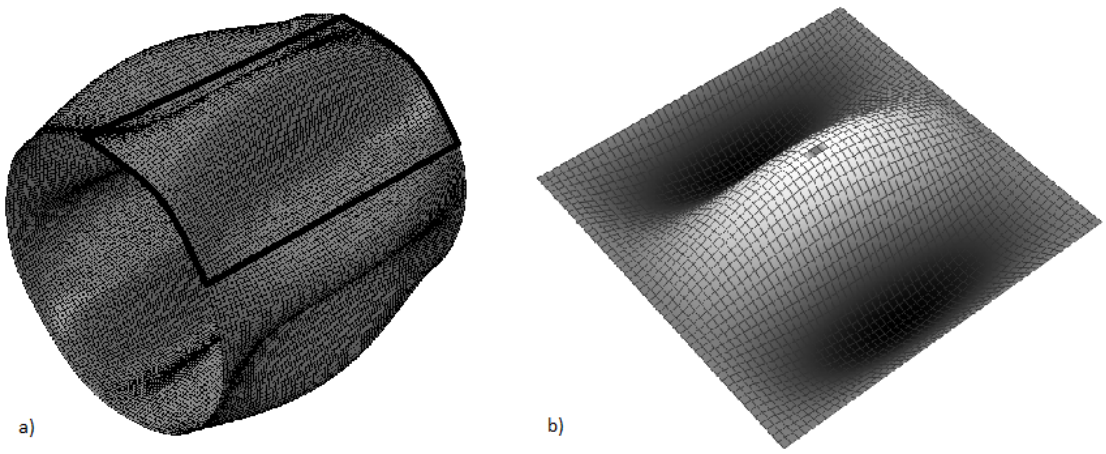

Figure 5.5: The buckling mode in a) Abaqus and b) Rayleigh Ritz of a cylindrical shell with L=4200, a=1900mm and t=14 subjected to lateral pressure.

The values calculated by the semi-analytical model and by the element model are following each other. Some of the small differences can be caused by the manual handling of the rotational springs in the semi-analytical model.

The buckling mode of a cylindrical shell subjected to lateral pressure is shown in Fig.(5.5). Unlike the buckling mode of an axially compressed cylinder the wavelength in both directions are in this case much longer. The buckling mode has one half wave in the axial direction and six complete waves in the circumferential direction. The wavelength in the longitudinal direction is of

the same length as the length of the shell and this is typical of a moderately imperfection-sensitive shell. When the thickness and the radius of the cylindrical shells are kept constant, hence the length is the only variable, the number of half waves in the circumferential direction diminishes as the length is increasing.

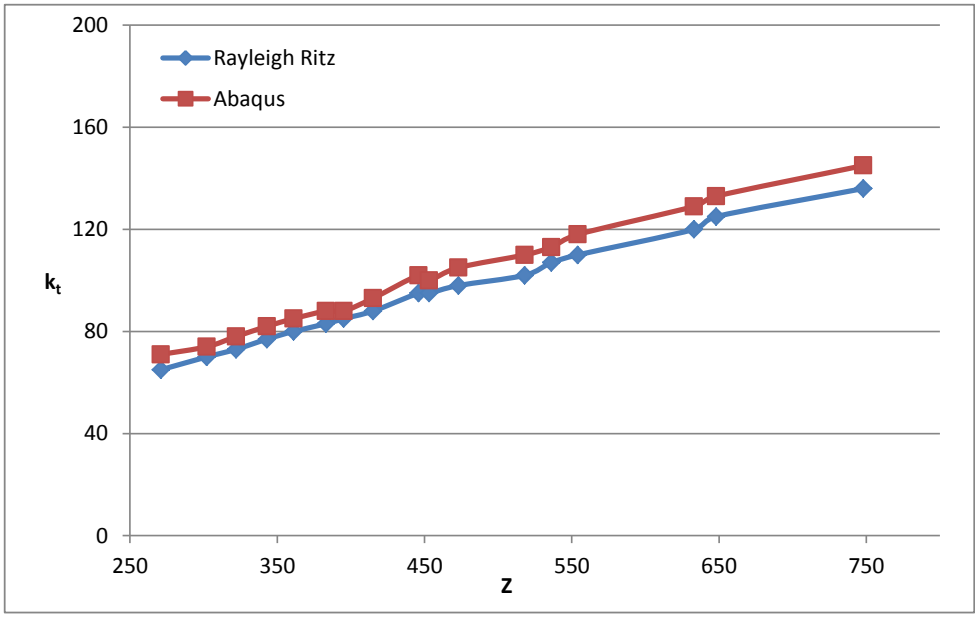

Figure 5.6: Critical values of shear stress for unstiffened cylindrical shells subjected to shear loading.

For a cylindrical shell subjected to a shear force, the parameter of the y-axis is given as:

$$k_t = \frac{L^2 t}{\pi^2 D}\tau_{cr} \tag{5.3.5}$$

where τ_{cr} is the critical shear load defined in (4.2.5). The Batdorf parameter Z is approaching zero as the radius a is moving toward infinity. From Fig. (5.6) it can be seen that the semi-analytical model is giving a lower buckling load than Abaqus when the shell is subjected to shear and the results from the semi-analytical model are conservative. As the length of the shell is increasing and the thickness of the shell is decreasing, the difference between the semi-analytical model and Abaqus is increasing. Also for a cylindrical shell subjected to a shear load, the higher order eigenvalues are not as

dense as with the axially loaded cylindrical shell, explaining why the curve in Fig.(5.6) is moving up and down as Z is increasing, the same as for a shell subjected to lateral pressure.

Fig.(5.7) is showing the buckling mode of a cylindrical shell subjected to a shear load, and by comparing one fourth of the shell from Abaqus with the buckling mode of the semi-analytical model, it can be seen that the shell buckles in the same manner for the two models.

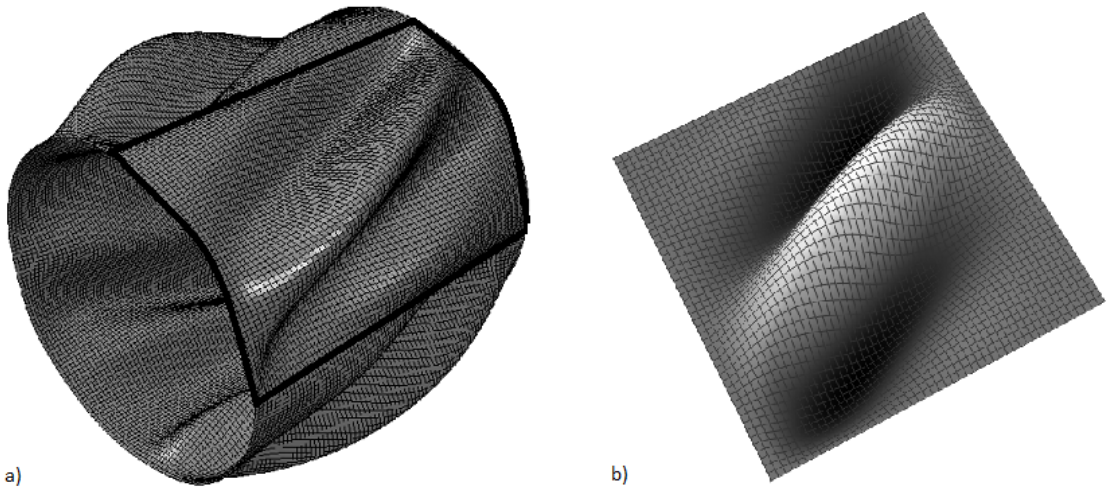

Figure 5.7: The buckling mode in a) Abaqus and b) Rayleigh Ritz of a cylindrical shell with L=4200mm, a=1900mm and t=14mm subjected to shear loading.

5.4 Ring stiffened shell

For the shell stiffened in the ring direction, one stiffener with the same material properties as the shell has been placed at $L/2$, see Fig(5.8), and analyses have been carried out on cylindrical shells of the same dimensional range as was described in the previous section and with the same types of loads.

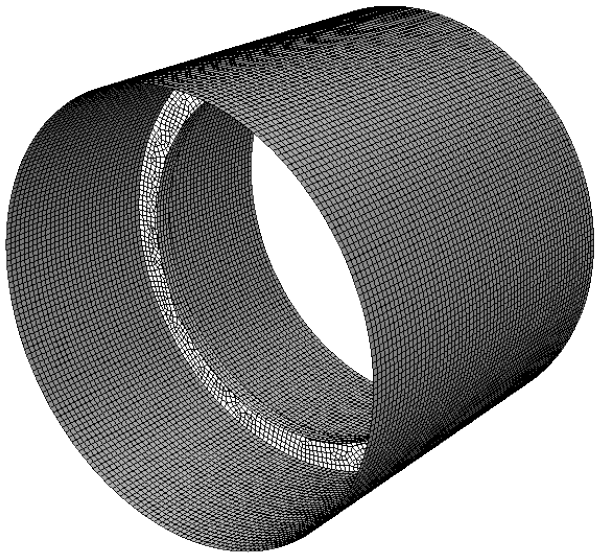

Figure 5.8: An element model of a cylindrical shell with an internal ring stiffener placed at $L/2$.

The T shaped ring stiffener has the following dimensions:

$$h_w{=}300 \quad t_w{=}15 \quad t_f = 20 \quad w_f = 150$$

In the semi-analytical model the moment of inertia of the ring stiffener is calculated about the shells mid surface The ring stiffeners moment of inertia about the shells midsurface is depending on the shape and the dimensions of the stiffener. For the T shaped ring stiffener shown in Fig.(5.9) the moment of inertia about its relevant centroidal axis is calculated as:

$$I = 79930000mm^4 \tag{5.4.1}$$

For a cylindrical shell subjected to an axial compressive load a ring stiffener

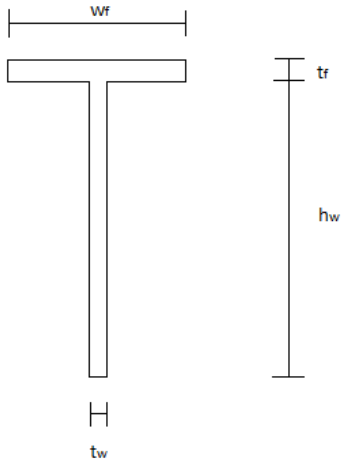

Figure 5.9: Shape and size of ring stiffener.

placed at $L/2$ is to a very little extend contributing to a greater support of the structure. This is because the shell loaded with axial compression is buckling into many small half waves and it is therefor difficult to place the ring stiffener in such a way that it will prevent the shell from buckling. Placing several ring stiffeners very close to each other and then smear them out for calculation can be done to achieve a higher buckling load. For this thesis the ring stiffeners are treated as discrete elements and with the number of stiffeners tried out on a cylindrical shell subjected to axial compression no appreciable increase in strength was achieved.

Fig.(5.10) is showing the results from the ring stiffened cylindrical shells subjected to lateral pressure. The results from the semi-analytical model are slightly higher than the results from Abaqus. The buckling mode of a ring stiffened shell subjected to lateral pressure can be seen in Fig.(5.11). The shell is buckling into one half wave on each side of the ring stiffener and eight complete waves in the ring direction.

Fig.(5.12) is showing the results from the ring stiffened cylindrical shells subjected to a shear load. The results from the two models are in good agreement with each other. Fig.(5.13) is showing how a shear loaded ring stiffened shell buckles.

In Fig.(5.14) the results from the unstiffened lateral pressured shell is shown together with the results from the ring stiffened lateral pressured shell. The ring stiffener at position $L/2$ makes the shell take on much more load before

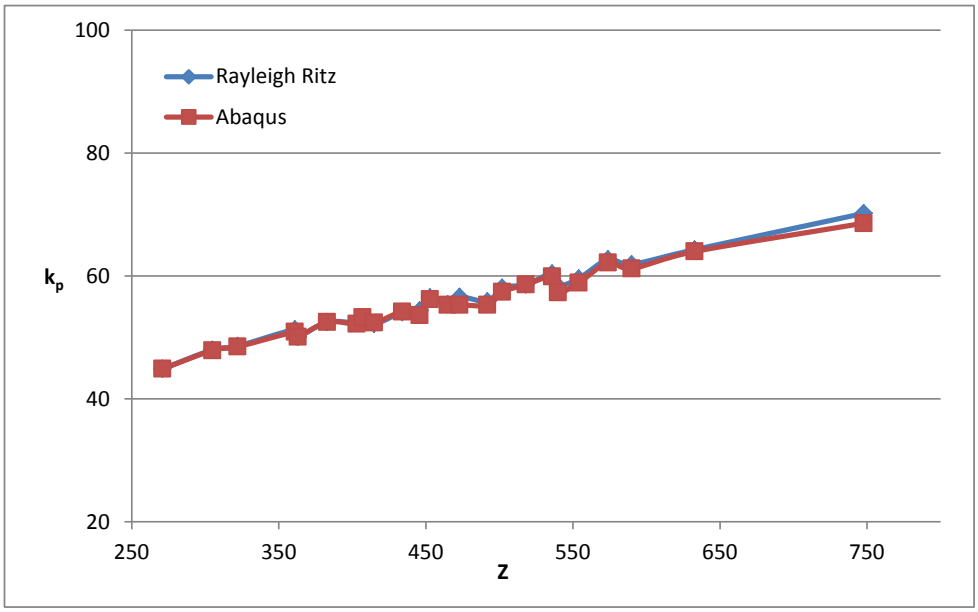

Figure 5.10: Critical values of pressure for ring stiffened cylindrical shells subjected to lateral pressure.

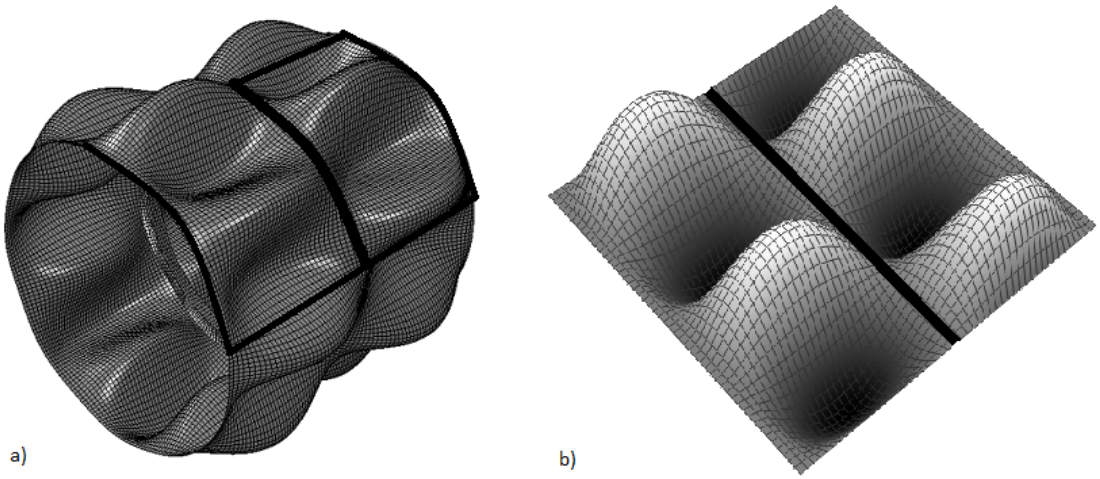

Figure 5.11: The buckling mode in a) Abaqus and b) Rayleigh Ritz of a ring stiffened cylindrical shell with L=4200mm, a=1900mm and t=14mm subjected to lateral pressure.

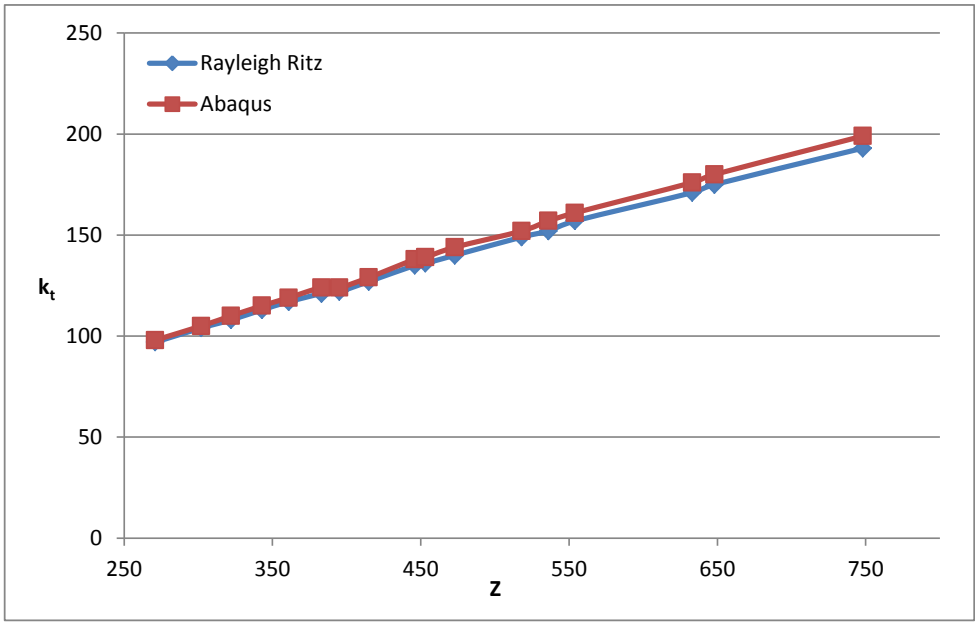

Figure 5.12: Critical values of shear stress for ring stiffened cylindrical shells subjected to shear loading.

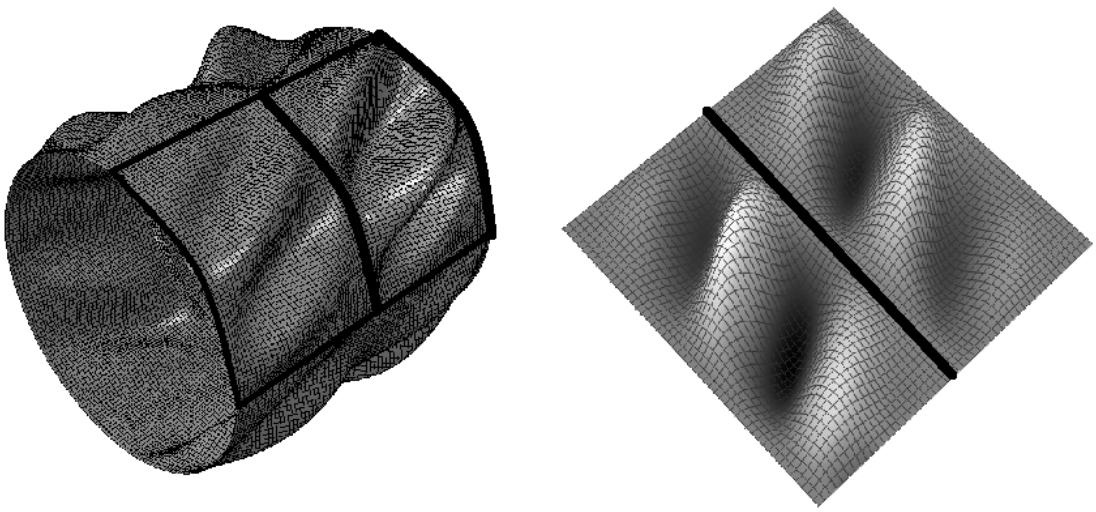

Figure 5.13: The buckling mode in a) Abaqus and b) Rayleigh Ritz of a ring stiffened cylindrical shell with L=4200mm, a=1900mm and t=14mm subjected to shear loading.

the shell buckles. As Z is increasing, the length L of the shell is increasing and the thickness t is decreasing, it can be seen that the ring stiffener has an increasing effect on the shell's resistance to buckling. The same is the case for a shell subjected to shear, see Fig.(5.15), where the percentage increase in how much load the shell can be exposed to before buckling is larger for a longer and thinner shell when the cylindrical shell is stiffened in the ring direction. Comparing the results from Fig.(5.14) and Fig.(5.15) shows that the ring stiffener has a better effect on a shell subjected to pressure than a shell subjected to shear. This is because of the ring's position, an oblique direction for the ring stiffener would for the shear loaded shell have an even better effect because of the direction of the buckling half waves of the shell.

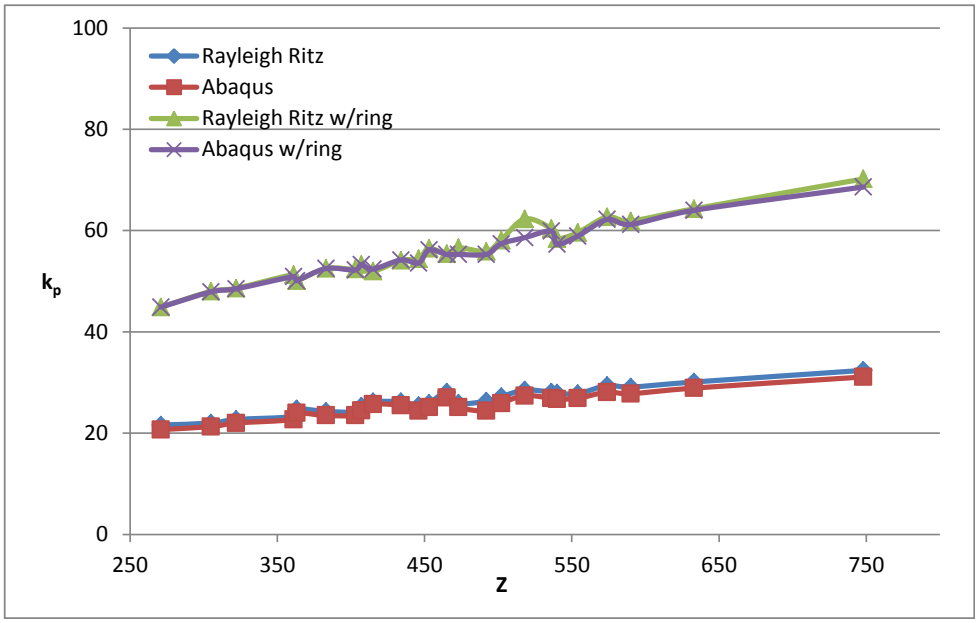

Figure 5.14: Effect of ring stiffener on cylindrical shells subjected to lateral pressure.

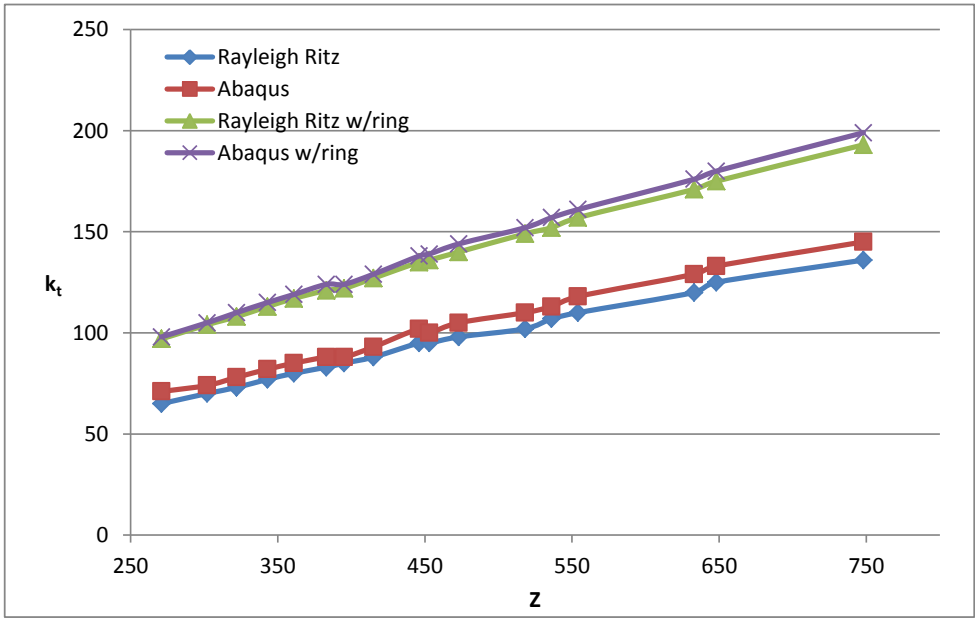

Figure 5.15: Effect of ring stiffener on cylindrical shells subjected to shear loading.

5.5 Stringer stiffened shell

For the shell stiffened in the longitudinal direction, the stiffeners have been placed at angles $\pi/4$, $3\pi/4$, $5\pi/4$ and $7\pi/4$ as can be seen in Fig.(5.16). The dimensions of the longitudinal stiffeners are the same as for the ring stiffener, the shape can be seen in Fig.(5.9) and the dimensions are found in Eq.(5.4). In addition, a constraint in the element model has been made for the nodes along the lines at angles $\pi/2$, π, $3\pi/2$ and 2π. The nodes are to move at an equal distance in the radial direction when the shell is loaded.

A stiffeners moment of inertia about a shell's midsurface is a big contribution to the bending stiffness of the stiffener. Depending on the thickness of the shell, the moment of inertia about the shells mid surface can be calculated.

For the same reason as with a ring stiffened cylindrical shell subjected to an axial compressive load, a longitudinal stiffened cylindrical shell subjected to the same type of loading is not showing a much greater increase in strength compared to an unstiffened cylindrical shell. The longitudinal stiffeners have

Figure 5.16: An element model of a cylindrical shell with internal stringer stiffeners placed at angles $\pi/4$, $3\pi/4$, $5\pi/4$ and $7\pi/4$.

an easiness of being placed between two half waves and radial displacement is hence not prevented. Placing the longitudinal stiffeners closely can lead to a greater buckling load. A cylindrical shell with closely spaced longitudinal stiffeners has not been further investigated in this thesis.

As was seen in the previous section, a ring stiffener placed at $L/2$ on a cylindrical shell subjected to lateral pressure made the shell stiffer and a higher buckling load was achieved. A cylindrical shell stiffened in the longitudinal direction and subjected to lateral pressure is not showing the same effect. This is because of the short half waves in the ring direction of the shell when it buckles. The longitudinal stiffeners are not making a great contribution to the stiffness of the structure because they, as with the axial loaded stiffened cylindrical shell, tend to end up between the buckling half waves.

The results for a cylindrical shell stiffened in the longitudinal direction and subjected to a shear load can be seen in Fig.(5.17). The longitudinal stiffeners are making the structure stiffer and an appreciable higher buckling load is achieved compared to what an unstiffened cylindrical shell could obtain. The analyses were carried out on shells with a length from $3200mm$ to

4400mm, the same range as earlier in the thesis. The radius is kept constant at 1900mm and the thickness vary from 13mm to 19mm.

A shell loaded with shear is also buckling into many short half waves in the ring direction, as was the case for a shell subjected to axial compression and a shell subjected to lateral pressure. Unlike the latter two, the half waves of a buckled shear loaded shell are at an angle from the direction of the longitudinal direction and the stiffeners can in that matter contribute better to a stiffer structure than what was the case with the stiffened shell subjected to axial compression and the stiffened shell subjected to lateral pressure.

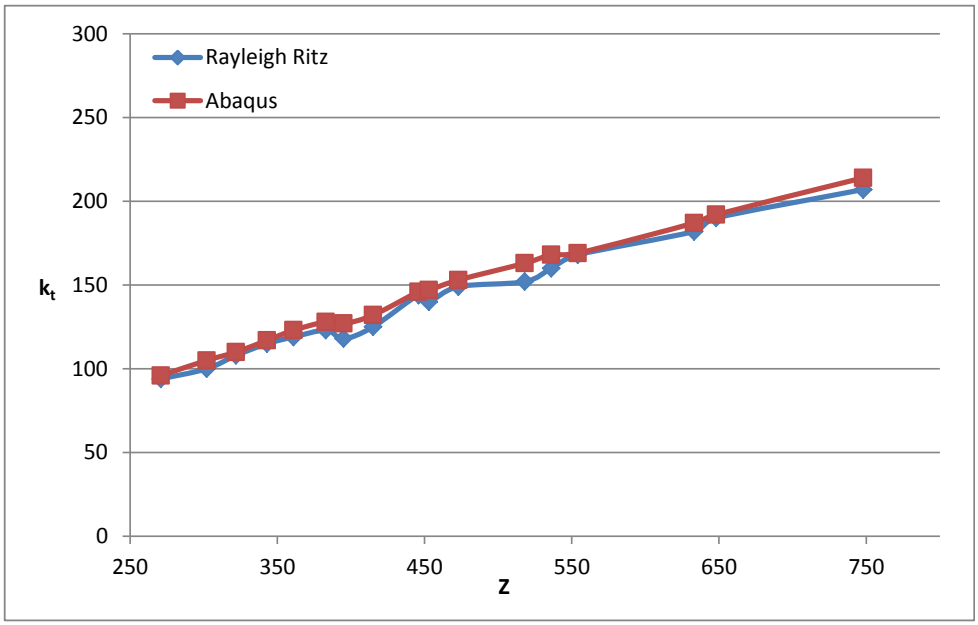

Figure 5.17: Critical values of shear stress for stringer stiffened cylindrical shells subjected to shear loading.

From the graph in Fig.(5.17) it can be seen that the results from the semi-analytical model and the results from Abaqus are in good agreement. The buckling mode of longitudinal stiffened shells subjected to a shear load can be seen in Fig.(5.18).

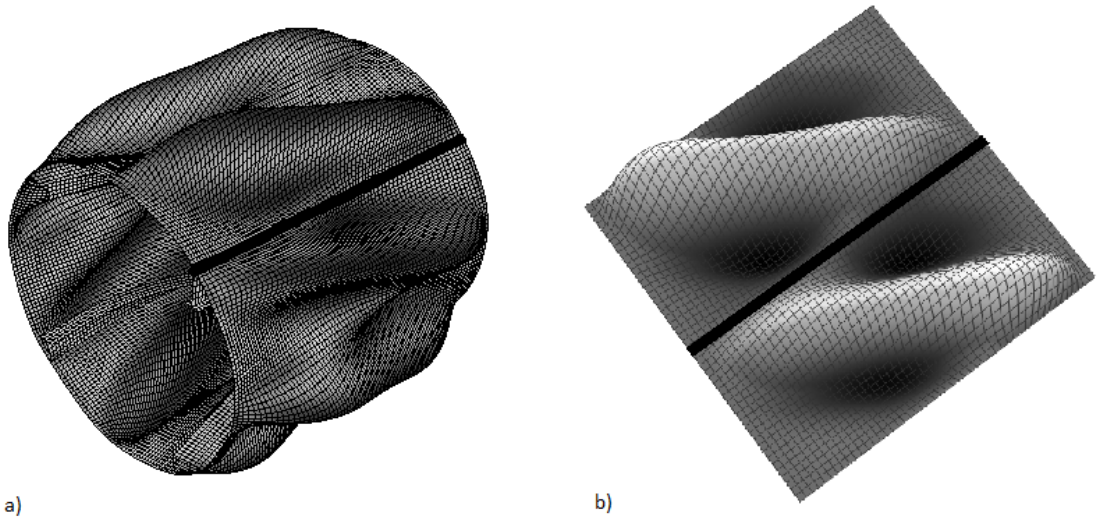

Figure 5.18: The buckling mode in a) Abaqus and b) Rayleigh Ritz of a stringer stiffened cylindrical shell subjected to shear loading.

Chapter 6

Apply of the shell model

6.1 Introduction

In this chapter the semi-analytical model has been compared to an element model describing a fourth of a cylindrical shell. This is the shape of a structure found in the transition from the side to the bottom of a ship. This type of structure is called a bilge. The semi-analytical model is based on Donnel's kinematic relations witch are valid for a complete cylinder and in chapter 5 the model was verified against a complete cylinder in Abaqus. The same loading as before has been subjected to the stiffened shell.

6.2 Comparing with an element model

The transition from the side of a ship to its bottom is called a bilge. A bilge very often has the shape as a fourth of a cylindrical shell and girders, frames and stiffeners are providing support to the structure. In the element model the edges in the circumferential direction are both being clamped. The edges are allowed to move in the radial direction when the shell is being subjected to different types of loads. Strong web frames in the longitudinal direction of the bilge are positioned where the ship side and the bilge meet and where the bottom of the ship and the bilge meet. It is normal for the edges along the frame lines to rotate. In the element model the edges in the longitudinal direction are simply supported and are held straight. The edges are constraint to move at an equal distance in the radial direction and held from moving in

the θ direction. Also the boundaries at $L = 0$ and $L = L_s$ are constraint to move an equal distance in the radial direction when the shell is subjected to a load, the same as for the element model of a complete cylinder. To prevent rigid body motion, one node at the element model is fixed in the longitudinal direction.

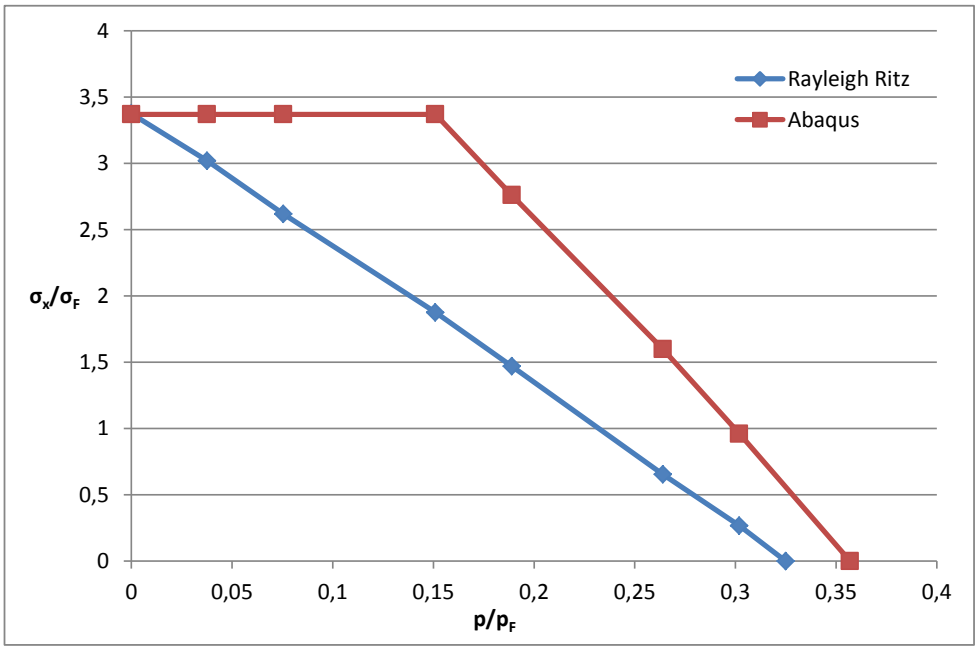

Figure 6.1: Interaction curves for a shell where $L = 3400mm$, $a = 1900mm$ and $t = 16mm$.

An interaction curve is made for the unstiffened shell. The shell is subjected to axial compression in combination with lateral pressure, where the lateral pressure is added as prestress with increasing magnitude. The dimensions of the shell studied are:

L=3400mm t=16mm a=1900mm

The yield stress of steel is $\sigma_F = 315MPa$, and p_F, which is the size of the external pressure when the stress in the ring direction is equal to the yield stress, can be defined through σ_F as:

$$p_F = \frac{t}{a}\sigma_F \tag{6.2.1}$$

The interaction curve can be seen in Fig.(6.1). The results from the semi-analytical model is very conservative in comparison with the element model. While a small magnitude of the prestress is affecting the result in the semi-analytical model and also the associated buckling mode, a larger prestress must be added in the element model for the same effect and also to change shell from buckling into short half waves to buckling into fewer and larger half waves. This difference is due to the edges in the longitudinal direction in the element model being held straight. This is making the element model stiffer. In reality, for a bilge, the result would be somewhere in between the two.

When the Batdorf parameter Z is relatively large, as is the case with the dimensions for the bilge studied in this thesis, the circumferential stress at which buckling occur under hydrostatic pressure is the same as when the shells are subjected to lateral pressure only. At high values of Z the axial stress required to produce buckling is many times the circumferential stress required and this is the reason for the circumferential stress to be the main factor in buckling at the given Z values [16]. The big difference in the results from the semi-analytical model and the element model in the interaction curve in Fig.(6.1) is thereby strongly dependent on the dimensions of the shell.

6.3 Unstiffened shell

Again the semi-analytic model has been used to analyze shells with a range in dimensions covering typical sizes of a bilge on a ship and comparing the results to the element model. The length is varying from $3200mm$ to $4400mm$ and the thickness is varying from $13mm$ to $19mm$. The radius is kept constant at $1900mm$. The shell has been subjected to axial compression, lateral pressure and shear loading, all contributing to uniform stress in the shell. The results are found graphically in Fig.(6.2), Fig.(6.3) and Fig.(6.4), respectively. The Batdorf parameter Z on the x-axis and the nondimensional parameters k_a, k_p and k_t representing the y-axis for every load situation are defined in chapter 5.

For the unstiffened shells subjected to axial compression the buckling load is the same as for complete cylindrical shells and the semi-analytical model is well-suited for this type of loading as can be seen in Fig.(6.2). For the two other load cases, lateral pressure and shear loading, the results from

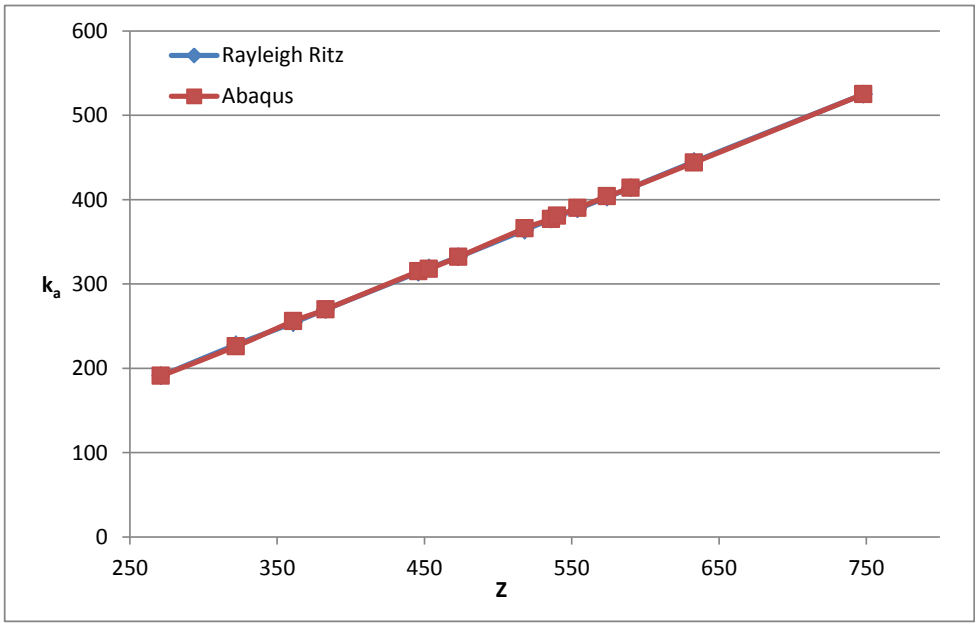

Figure 6.2: Critical values of axial stress for unstiffened cylindrical shells subjected to axial compression.

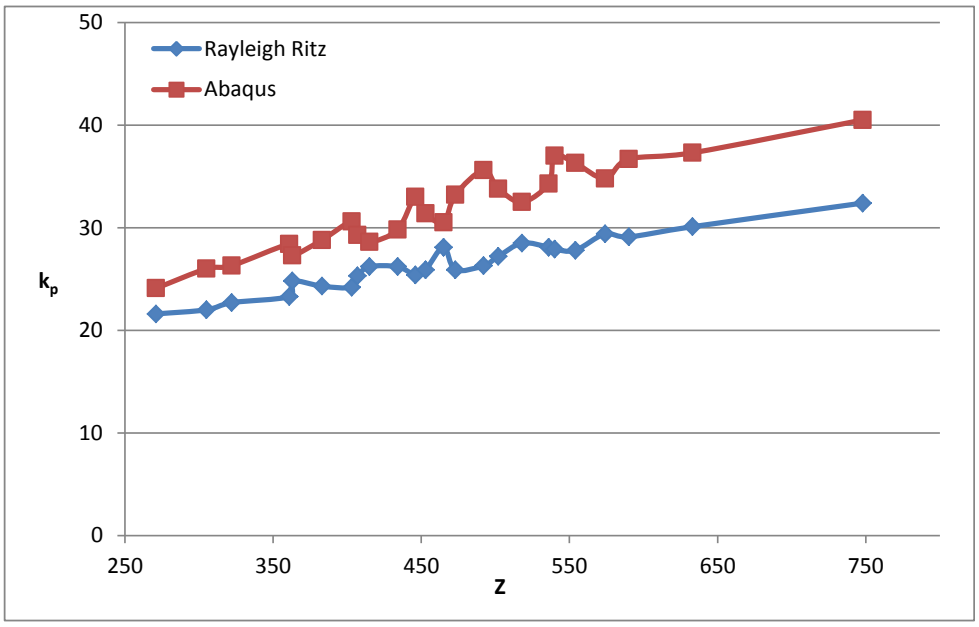

Figure 6.3: Critical values of pressure for unstiffened cylindrical shells subjected to lateral pressure.

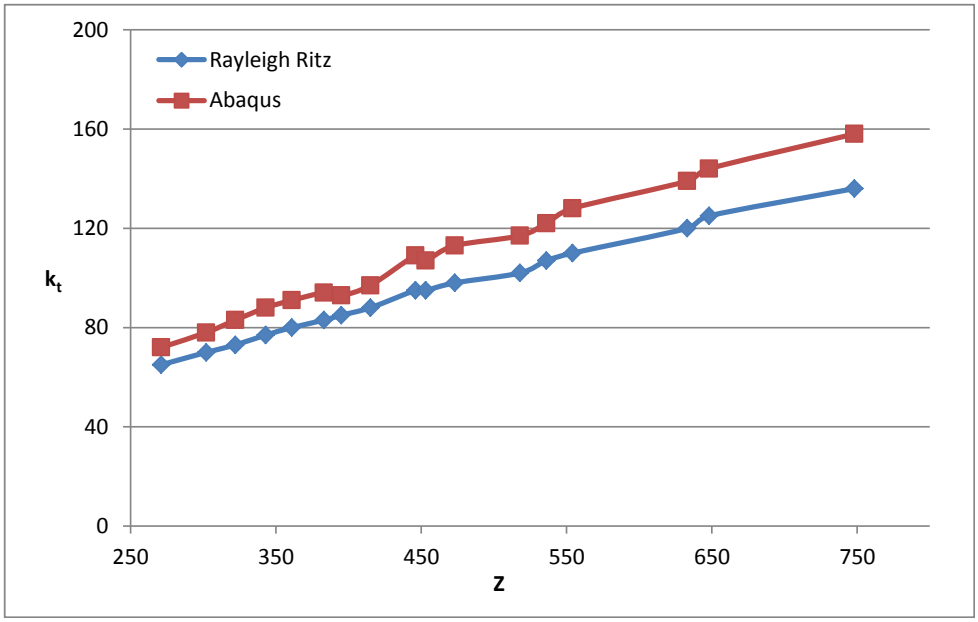

Figure 6.4: Critical values of shear stress for unstiffened cylindrical shells subjected to shear loading.

the model and the element model are more deviating, with the results from the semi-analytical model being more conservative in both cases. The shell subjected to lateral pressure is showing the biggest difference in the results. In the element model the edges are held straight and this is contributing to a stiffer model and is explaining the difference between the results from the semi-analytical model and the results from the element model. The constraint on the edges and at the boundaries does not affect the shell subjected to axial compression because the shell buckles into many small halfwaves in both directions.

Again, the graph for the shells subjected to lateral pressure and to a shear load are moving up and down as Z is increasing, while the graph for the shell subjected to axial compression is an almost straight line.

6.4 Ring stiffened shell

As was described in chapter 5, a ring stiffener placed at $L/2$ did not contribute to a higher stiffness in a shell subjected to axial compression. In this chapter only ring stiffened shells subjected to lateral pressure and a shear load in the semi- analytical model has been tried out and compared to an element model. The result can be seen in Fig.(6.5) for the shells subjected to lateral pressure and in Fig.(6.6) for the shells subjected to shear loading. In both cases the results from Abaqus are higher than the results from the semi analytical model, where the largest difference is again found in the stiffened shell subjected to lateral pressure. Comparing with the unstiffened shell, this difference between the results is lesser for the ring stiffened shell. The ring stiffener is dividing the shell into two parts and keeping the edges straight is not having the same effect for a shorter shell.

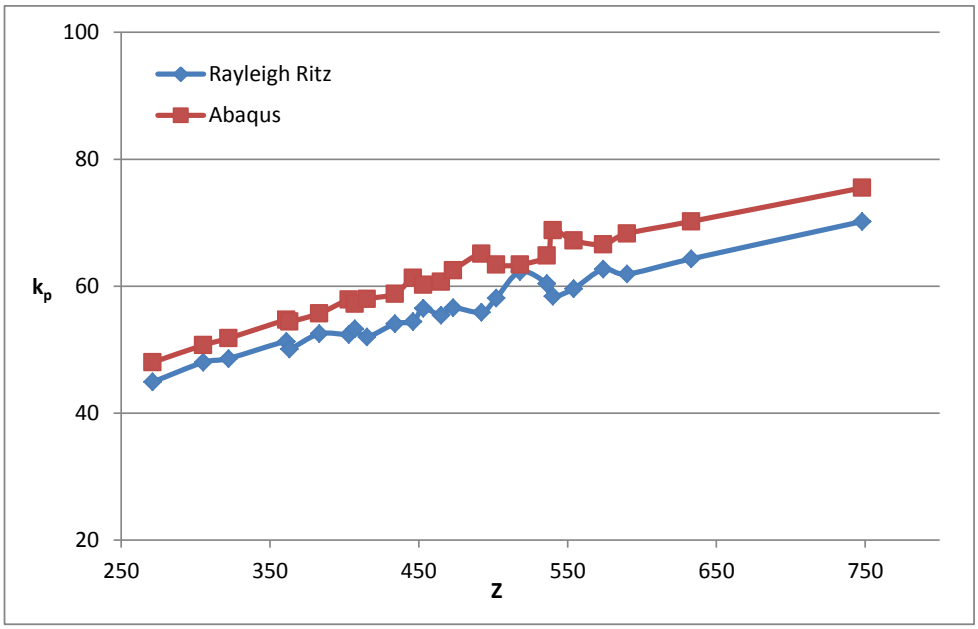

Figure 6.5: Critical values of pressure for ring stiffened cylindrical shells subjected to lateral pressure.

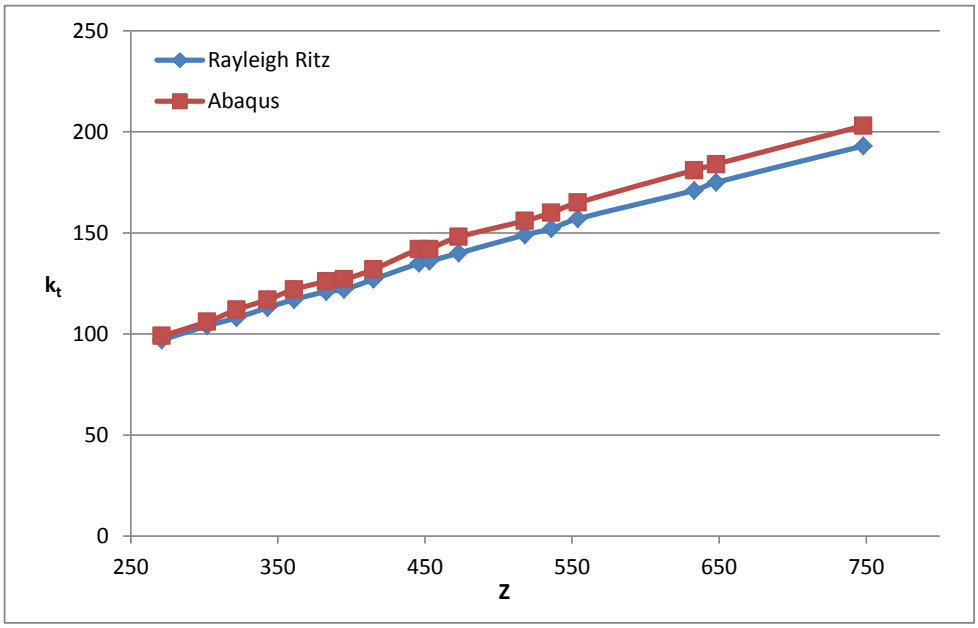

Figure 6.6: Critical values of shear stress for ring stiffened cylindrical shells subjected to shear loading.

6.5 Stringer stiffened shell

When the cylindrical shell is subjected to shear the edges at $\theta = 0$ and $\theta = \pi/2$ are forced to move along a straight line in the element model. This is causing a stiffer system and Fig.(6.7) is showing the results from the stringer stiffened shells subjected to a shear load. The result from the element model are higher than the results from the semi-analytical model as expected due to the boundary conditions.

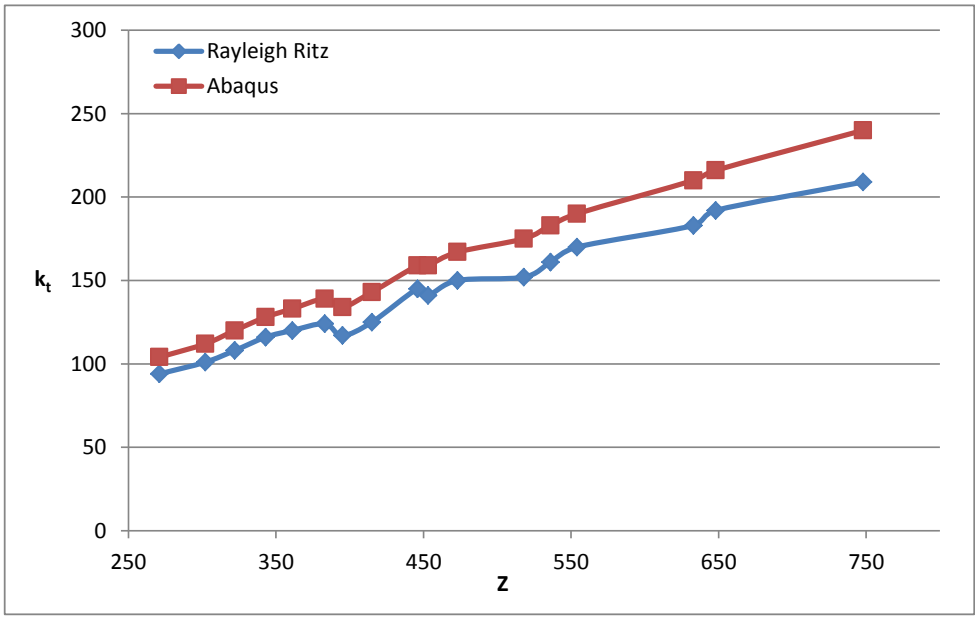

Figure 6.7: Critical values of shear stress for stringer stiffened cylindrical shells subjected to shear loading.

Chapter 7

Summary and conclusion

7.1 Introduction

In this thesis a semi-analytical model for eigenvalue calculations of stiffened cylindrical shells has been made. This shell is describing the rounded portion forming a transition between the bottom and the side of a ship's hull, known as a bilge. Cylindrical shells with stiffeners in both the ring direction and the longitudinal direction can be analyzed by the model. The stiffeners are treated as discrete elements and are assumed to behave as beam elements. The bending stiffness of the stiffeners is freely chosen in the model. The clamped shell can be subjected to axial compression, lateral pressure and shear loading.

The semi-analytical model is based on the Rayleigh-Ritz method. In short, the Rayleigh-Ritz method is assuming a displacement field to describe the deformation of a structure. The displacement field is a sum of linear independent shape functions in combination with undetermined coefficients, and it is defined throughout the structure. The shape functions must satisfy compatibility conditions and essential boundary conditions. The displacement that makes the potential energy stationary is to be found. The buckling load and the associated buckling mode is found from the calculation of the stationary potential energy.

A strain energy expression for a ring stiffener and a strain energy expression for a longitudinal stiffener has been found in this thesis. In the eigenvalue calculation the stiffness of the stiffeners are added to the material stiffness.

The finite element analysis software Abaqus has been used to verify the semi-analytical model. The buckling load of a clamped shell or a shell subjected to shear cannot be found analytically and the element program is very useful for comparison of the results. In this thesis many analyses has been performed for a variety of shell dimensions. An unstiffened shell was first verified, then a ring stiffened shell and finally a stringer stiffened shell. The results from the semi-analytical model and from the element model were generally in agreement with each other. With the apply of the shell model larger difference between the semi-analytical model and the element model was found. This difference in the results was mainly due to a slight difference in the boundary conditions in the element model compared with the semi-analytical model. For a real structure the answer would lay somewhere in between the two. A higher buckling load was found in the element model due to a stiffer model, hence the semi-analytical model is conservative.

7.2 Semi-analytical model

The semi-analytical model was compared with an element model describing the transition from a ship's side to its bottom. The edges in the longitudinal direction were held straight in the element model. This was done to describe no deformations as girders and frames in a real ship structure are preventing this. Comparison of results from the two models showed a higher buckling load in the element model. This was because of the edges being held straight, hence causing a stiffer model.

A ring stiffener was providing support to the shells subjected to lateral pressure and shear. For a ring stiffened shell subjected to axial compression no appreciable increase in strength was achieved. This was because of the short half waves in both the longitudinal direction and ring direction of the buckled shell making it difficult for the ring stiffener to prevent deformation. The results from the element model and the semi-analytical model were in good agreement for the ring stiffened shell. For the apply of the ring stiffened shell model, the results in the element model were again higher, but the difference was lesser than for an unstiffened shell. The ring stiffened shell can be compared with a short shell because of the stiffener, and keeping the edges straight in the element model, hence making the structure stiffer, is not having the same effect for a short shell. The results from the semi-analytical model were on the conservative side.

The stringer stiffener had a great effect on the shell subjected to shear. While shells subjected to axial compression and lateral pressure buckles into short half waves in the ring direction a stringer stiffener has difficulties supporting the shell just like the ring stiffener on a shell subjected to axial compression. An oblique direction of the buckling half waves of a shear loaded shell makes the stringer having an effect on the buckling load. For the apply of the stringer stiffened shell model a higher buckling load was found in the element model. This was because of the constraint on the edges. Again, the results from the semi-analytical model were on the conservative side.

7.3 Suggestions for further work

The semi-analytical model developed in this thesis can be improved and developed forth for wider use. Suggestions for further work are:

- The stiffeners can be developed forth to include torsional stiffness. This is particularly relevant for stiffeners with a closed profile. The potential energy due to the torsional stiffness is to be included in the principle of stationary energy.
- Develop a non-linear shell model for buckling analyses valid for large deformations.
- Estimate a stiffened shell's capacity, either by using eigenvalues and an empirical formula or by using a non-linear model.
- Extend the shell model so that bending moment can be subjected to the shell. With a bending moment the stress is varying along the edges, which is a common situation for among other things fuel tanks.

Bibliography

[1] Ramm, E. and Wall, W.A. (2004) *Shell Structures - A Sensitive Interrelation between Physics and Numerics* [Online] Available at: http://shellbuckling.com/papers/2004ramm.pdf (Accessed: 15 May 2013).

[2] Bushnell, D. (1981) 'Buckling of Shells-Pitfall for Designers', *AIAA Journal*, 19(9), p. 1183-1226.

[3] Brush, D.O. and Almroth, B.O. (1975) *Buckling of Bars, Plates, and Shells*. New York: Mcgraw-Hill Book Company, Inc.

[4] Bushnell, D. (1984) 'Computerized analysis of shells-governing equations', *Computers and structures*, 18(3), p. 471-536.

[5] Bergan, P.G. and Syvertsen, T.G. (1989) *Knekning av Søyler og Rammer*. 2nd ed. Trondheim: Tapir trykk.

[6] Cook, R.D. et al. (2002) *Concepts and Application of Finite Element Analysis*. 4th ed. New Jersey: John Wiley & Sons, Inc.

[7] Reddy, J.N. (2002) *Energy Principles and Variational Methods in Applied Mechanics*. 2nd ed. New Jersey: John Wiley & Sons, Inc.

[8] Timoshenko, S.P. and Goodier, J.N. (1951) *Theory of Elasticity*. New York: Mcgraw-Hill Book Company, Inc.

[9] Ventsel, E. and Krauthammer, T. (2001) *Thin Plates and Shells. Theory, Analysis, and Applications*. 1st ed. New York: Taylor & Francis.

[10] Bushnell, D. (2011) *Imperfection sensitivity* [Online] Available at: http://shellbuckling.com/papers/imperfsensitivity.pdf (Accessed: 20 November 2012).

[11] Falzon, G.B. and Hitchings, D. (2006) *An Introduction to Modelling Buckling and Collapse*. 2nd ed. NAFEMS.

[12] Abaqus. (1998) *Analysis User's Manual, Version 6.12*. Rhode Island: Hibbitt, Karlsson and Sorensen, inc. USA

[13] Det Norske Veritas. (2009) *Non-Linear Finite Element Collapse Analyses of Stiffened Panels. Procedure Description*. Det Norske Veritas, Veritasveien 1, N-1322 Høvik, Norway.

[14] Timoshenko, S.P. and Gere, J.M (1963) *Theory of Elastic Stability*. New York: Mcgraw-Hill Book Company, Inc.

[15] Brubak, L. (2003) *Knekning av plater og skall i skipskontruksjoner*. Master thesis. University of Oslo, Oslo.

[16] Batdorf, S.B. (1947) *A simplified method of elastic-stability analysis for thin cylindrical shells* NACA Rep. 874.

Appendix A

Buckling of shells

A.1 Differentiated series expressions

The differentiated series expressions of the stress function f found in (A.2.2) are as follows:

$$\begin{aligned}
\frac{\partial^2 f}{\partial x^2} &= -\frac{1}{a^2} S_\theta - \sum_{i=1}^{m}\sum_{j=1}^{n} f_{ij}^S \left(\frac{\pi i}{L}\right)^2 \sin\left(\frac{\pi i}{L}x\right)\sin(2j\theta) \\
\frac{\partial^2 f}{\partial \theta^2} &= -S_x - \sum_{i=1}^{m}\sum_{j=1}^{n} f_{ij}^S (2j)^2 \sin\left(\frac{\pi i}{L}x\right)\sin(2j\theta) \\
\frac{\partial^2 f}{\partial x \partial \theta} &= \frac{1}{a} S_{x\theta} + \sum_{i=1}^{m}\sum_{j=1}^{n} f_{ij}^S \frac{\pi i}{L} 2j \cos\left(\frac{\pi i}{L}x\right)\cos(2j\theta)
\end{aligned} \tag{A.1.1}$$

By differentiation, the derivatives and higher order derivatives of the assumed displacement function w involved in the calculation of potential energy are:

$$\begin{aligned}
\frac{\partial w}{\partial x} &= \sum_{i=1}^{m}\sum_{j=1}^{n} a_{ij}\frac{\pi i}{L}\cos\left(\frac{\pi i}{L}x\right)\sin(2j\theta) \\
\frac{\partial w}{\partial \theta} &= \sum_{i=1}^{m}\sum_{j=1}^{n} a_{ij}2j\sin\left(\frac{\pi i}{L}x\right)\cos(2j\theta) \\
\frac{\partial^2 w}{\partial x^2} &= \sum_{i=1}^{m}\sum_{j=1}^{n} -a_{ij}\left(\frac{\pi i}{L}\right)^2\sin\left(\frac{\pi i}{L}x\right)\sin(2j\theta) \\
\frac{\partial^2 w}{\partial \theta^2} &= \sum_{i=1}^{m}\sum_{j=1}^{n} -a_{ij}(2j)^2\sin\left(\frac{\pi i}{L}x\right)\sin(2j\theta) \\
\frac{\partial^2 w}{\partial x \partial \theta} &= \sum_{i=1}^{m}\sum_{j=1}^{n} a_{ij}\frac{\pi i}{L}2j\cos\left(\frac{\pi i}{L}x\right)\cos(2j\theta) \\
\frac{\partial^3 w}{\partial x^3} &= \sum_{i=1}^{m}\sum_{j=1}^{n} -a_{ij}(\frac{\pi i}{L})^3\cos\left(\frac{\pi i}{L}x\right)\sin(2j\theta) \\
\frac{\partial^3 w}{\partial x^2 \partial \theta} &= \sum_{i=1}^{m}\sum_{j=1}^{n} -a_{ij}\left(\frac{\pi i}{L}\right)^2 2j\sin\left(\frac{\pi i}{L}x\right)\cos(2j\theta) \\
\frac{\partial^3 w}{\partial x \partial \theta^2} &= \sum_{i=1}^{m}\sum_{j=1}^{n} -a_{ij}\frac{\pi i}{L}(2j)^2\cos\left(\frac{\pi i}{L}x\right)\sin(2j\theta)
\end{aligned} \tag{A.1.2}$$

A.2 Airy's stress function

For a cylindrical shell the compatibility equation is written as:

$$\nabla^4 f = \frac{E}{a^4}(w_{,x\theta}^{2} - w_{,xx}\, w_{,\theta\theta} + a w_{,xx}) \tag{A.2.1}$$

The solution to equation (A.2.1) with the assumed displacement function in (4.2.1) has been calculated in [15] and can be written as:

$$\begin{aligned} f(x,\theta) = &-\frac{1}{2a^2}S_\theta x^2 - \frac{1}{2}S_x\theta^2 + \frac{1}{a}S_{x\theta}x\theta \\ &+ \sum_{i=1}^{m}\sum_{j=1}^{n} f_{ij}^S \sin\left(\frac{\pi i}{L}x\right)\sin(2j\theta) \\ &+ \sum_{i=0}^{2m}\sum_{j=0}^{2n} f_{ij}^C \cos\left(\frac{\pi i}{L}x\right)\cos(2j\theta) \end{aligned} \tag{A.2.2}$$

By substituting Eq.(A.2.2) into the compatibility equation, the coefficients f_{ij}^S and f_{ij}^C are obtained. For the shell the following equation results:

$$\begin{aligned} &\frac{1}{a^4}\sum_{i=1}^{m}\sum_{j=1}^{n} f_{ij}^S \left[\left(\frac{\pi i}{L}\right)^2 + \left(\frac{2j}{a}\right)^2\right]^2 \sin\left(\frac{\pi i}{L}x\right)\sin(2j\theta) \\ &+ \sum_{i=0}^{2m}\sum_{j=0}^{2n} f_{ij}^C \left[\left(\frac{\pi i}{L}\right)^2 + \left(\frac{2j}{a}\right)^2\right]^2 \cos\left(\frac{\pi i}{L}x\right)\cos(2j\theta) \\ &= \frac{E}{a^4}\left[\sum_{rspq} a_{rs}a_{pq}\left(\frac{\pi r}{L}\right)(2s)\left(\frac{\pi p}{L}\right)(2q)\cos\left(\frac{\pi r}{L}x\right)\cos(2s\theta)\cos\left(\frac{\pi p}{L}x\right)\cos(2q\theta)\right. \\ &- \sum_{rspq} a_{rs}a_{pq}\left(\frac{\pi r}{L}\right)(2s)\left(\frac{\pi p}{L}\right)(2q)\sin\left(\frac{\pi r}{L}x\right)\sin(2s\theta)\sin\left(\frac{\pi p}{L}x\right)\sin(2q\theta) \\ &\left.- a\sum_{rs} a_{rs}\left(\frac{\pi r}{L}\right)^2 \sin\left(\frac{\pi r}{L}x\right)\sin(2s\theta)\right] \end{aligned} \tag{A.2.3}$$

By using trigonometric identities, the right hand side of (A.2.3) can be written as:

$$\begin{aligned}
\frac{2E\pi^2}{a^4L^2}\Bigg[&\sum_{rspq} rspqa_{rs}a_{pq}(\cos\left(\frac{(r-p)\pi x}{L}\right)\cos(2(s-q)\theta) \\
&+\cos\left(\frac{(r-p)\pi x}{L}\right)\cos(2(s+q)\theta)+\cos\left(\frac{(r+p)\pi x}{L}\right)\cos(2(s-q)\theta) \\
&+\cos\left(\frac{(r+p)\pi x}{L}\right)\cos(2(s+q)\theta)) \\
&-\sum_{rspq} r^2s^2a_{rs}a_{pq}(\cos\left(\frac{(r-p)\pi x}{L}\right)\cos(2(s-q)\theta) \\
&-\cos\left(\frac{(r-p)\pi x}{L}\right)\cos(2(s+q)\theta)-\cos\left(\frac{(r+p)\pi x}{L}\right)\cos(2(s-q)\theta) \\
&+\cos\left(\frac{(r+p)\pi x}{L}\right)\cos(2(s+q)\theta))-\frac{a}{2}\sum_{rs} r^2a_{rs}\sin\left(\frac{\pi r}{L}x\right)\sin(2s\theta)\Bigg]
\end{aligned} \tag{A.2.4}$$

For equation (A.2.3) to be true, the coefficients f_{ij}^S and f_{ij}^C must be:

$$\begin{aligned}
f_{ij}^S &= \frac{E\left(\frac{\pi r}{L}\right)^2}{a^3\left[\left(\frac{\pi i}{L}\right)^2+\left(\frac{2j}{a}\right)^2\right]^2}a_{rs} \\
f_{ij}^C &= \frac{E\left(\frac{\pi}{L}\right)^2}{\left[\left(\frac{\pi ia}{L}\right)^2+(2j)^2\right]^2}\sum_{rspq} b_{rspq}a_{rs}a_{pq}
\end{aligned} \tag{A.2.5}$$

where f_{00}^C is defined to be zero and the coefficients b_{rsbq} are:

$$b_{rspq} = rspq + r^2q^2 \qquad ,if\begin{cases}\pm(r-p)=i & ,s+q=j\\ r+p=i & ,\pm(s-q)=j\end{cases} \tag{A.2.6}$$

$$b_{rspq} = rspq - r^2q^2 \qquad ,if\begin{cases}r+p=i & ,s+q=j\\ \pm(r-p)=i & ,\pm(s-q)=j\end{cases} \tag{A.2.7}$$

The displacements in linearized second order theory are small and components including the amplitude a_{ij} to the second power are neglected and the solution to Eq.(A.2.1) can be written::

$$\begin{aligned}
f(x,\theta) = &-\frac{1}{2a^2}S_\theta x^2-\frac{1}{2}S_x\theta^2+\frac{1}{a}S_{x\theta}x\theta \\
&+\sum_{i=1}^{m}\sum_{j=1}^{n} f_{ij}^S\sin\left(\frac{\pi i}{L}x\right)\sin(2j\theta)
\end{aligned} \tag{A.2.8}$$

A.3 Shell membrane energy

The potential energy due to membran stretching is:

$$\begin{aligned} U^m_{shell} &= \frac{1}{2}\int_\theta\int_L \left(N_x\varepsilon^m_x + N_\theta\varepsilon^m_\theta + N_{x\theta}\varepsilon^m_{x\theta}\right) a dx d\theta \\ &= \frac{aC}{2}\int_0^{\frac{\pi}{2}}\int_0^L \left[(\varepsilon^m_x+\varepsilon^m_\theta)^2 - 2(1-\nu)(\varepsilon^m_x\varepsilon^m_\theta - (\varepsilon^m_{x\theta})^2)\right] dx d\theta \end{aligned} \tag{A.3.1}$$

By substitution of the stress function, the integration can be carried out:

$$\begin{aligned} U^m_{shell} =& \frac{Et\pi L}{16a}\sum_{i=1}^m\sum_{j=1}^n a_{ij}a_{ij}\frac{\left(\frac{\pi i}{L}\right)^4}{\left[\left(\frac{\pi i}{L}\right)^2+\left(\frac{2j}{a}\right)^2\right]^2} \\ &+\frac{a\pi L}{4Et}\left[(S_x+S_\theta)^2 - 2(1-\nu)(S_xS_\theta - S^2_{x\theta})\right] \end{aligned} \tag{A.3.2}$$

By differentiation, the stationary energy is:

$$\frac{\partial^2 U^m_{shell}}{\partial a_{ij}\partial a_{kl}} = \frac{Et\pi L}{8a}\frac{\left(\frac{\pi i}{L}\right)^4}{\left[\left(\frac{\pi i}{L}\right)^2+\left(\frac{2j}{a}\right)^2\right]^2} \tag{A.3.3}$$

A.4 Shell bending energy

The potential energy due to bending is:

$$\begin{aligned} U^b_{shell} &= \frac{1}{2}\int_\theta\int_L \left(M_x\kappa_x + M_\theta\kappa_\theta + M_{x\theta}\kappa_{x\theta}\right) a dx d\theta \\ &= \frac{aD}{2}\int_0^{\frac{\pi}{2}}\int_0^L \left[\left(w_{,xx}+\frac{w_{,\theta\theta}}{a^2}\right)^2 - 2(1-\nu)\left(w_{,xx}\frac{w_{,\theta\theta}}{a^2} - \frac{w^2_{,x\theta}}{a^2}\right)\right] dx d\theta \end{aligned} \tag{A.4.1}$$

By substitution of the assumed displacement function, the integration can be carried out:

$$U^b_{shell} = \frac{aD\pi L}{16}\sum_{i=1}^m\sum_{j=1}^n a_{ij}a_{ij}\left[\left(\frac{\pi i}{L}\right)^2+\left(\frac{2j}{a}\right)^2\right]^2 \tag{A.4.2}$$

By differentiation, the stationary energy is:

$$\frac{\partial^2 U^b_{shell}}{\partial a_{ij}\partial a_{kl}} = \frac{aD\pi L}{8}\left[\left(\frac{\pi i}{L}\right)^2+\left(\frac{2j}{a}\right)^2\right]^2 \tag{A.4.3}$$

A.5 Ring stiffener

The strain energy due to a ring stiffener is:

$$U^R = \frac{2EI_{0r}}{a^3} \int_0^{\frac{\pi}{2}} (w - w_{,\theta\theta})^2 d\theta \tag{A.5.1}$$

By substituting of the assumed displacement function, and integrating, the result is:

$$U^R = \frac{EI_{0r}\pi}{2a^3} \sum_{i=1}^{m} \sum_{j=1}^{n} a_{ij} a_{ij} \left(1 + (2j)^2\right)^2 \sin\left(\frac{\pi i}{L} x\right) \sin\left(\frac{\pi p}{L} x\right) \delta_{j,q} \tag{A.5.2}$$

By differentiation, the stationary energy is:

$$\frac{\partial^2 U^R}{\partial a_{ij} \partial_{kl}} = \frac{EI_{0r}\pi}{a^3} \left(1 - (2j)^2\right)^2 \sin\left(\frac{\pi i}{L}\right) \sin\left(\frac{\pi p}{L}\right) \delta_{j,q} \tag{A.5.3}$$

A.6 Longitudinal stiffener

The strain energy due to a longitudinal stiffener is:

$$U^L = \frac{EI_{0l}}{2} \int_0^L w_{,xx}^2 \, dx \tag{A.6.1}$$

By substituting of the assumed displacement function, and integrating, the result is:

$$U^L = \frac{EI_{0l}\pi^4}{4L^3} \sum_{i=1}^{m} \sum_{j=1}^{n} a_{ij} a_{ij} i^4 \sin(2j\theta) \sin(2q\theta) \delta_{i,p} \tag{A.6.2}$$

By differentiation, the stationary energy is:

$$\frac{\partial^2 U^L}{\partial a_{ij} \partial_{kl}} = \frac{EI_{0l}\pi^4}{4L^3} i^4 \sin(2j\theta) \sin(2q\theta) \delta_{i,p} \tag{A.6.3}$$

A.7 External energy

A.7.1 Potential energy due to axial stresses

The potential energy due to an axial force is:

$$T_{S_x} = \int_0^{\frac{\pi}{2}} S_x t \triangle u(\theta) a \, d\theta \tag{A.7.1}$$

where the elongation in the x-direction is:

$$\triangle u = \int_0^L u_{,x}\, dx = \int_0^L \left(\varepsilon_x - \frac{1}{2} w_{,x}^2\right) dx \tag{A.7.2}$$

Using hooke's law and the stress function, the membrane strain can be written as:

$$\begin{aligned}\varepsilon_x =& \frac{1}{E}(\sigma_x - \nu\sigma_y) \\ =& \frac{1}{E}\left(-S_x - \sum_{i=1}^{m}\sum_{j=1}^{n} f_{ij}^S \sin\left(\frac{\pi i}{L}x\right)(2j)^2 \sin(2j\theta)\right. \\ & \left. -\nu a^2\left(-\frac{S_\theta}{a^2} - \sum_{1=1}^{m}\sum_{j=1}^{n} f_{ij}^S \sin(2j\theta)\left(\frac{\pi i}{L}\right)^2 \sin\left(\frac{\pi i}{L}x\right)\right)\right)\end{aligned} \tag{A.7.3}$$

Substituting the above relation into (A.7.2), using the assumed displacement function in Eq.(4.2.1) and integrating gives the potential energy due to axial stress:

$$T_{S_x} = \sum_{i=1}^{m}\sum_{j=1}^{n} \frac{S_x taL\pi}{16}\left(\frac{\pi i}{L}\right)^2 a_{ij}a_{ij} - \frac{taL\pi}{2E}S_x^2 + \frac{\nu taL\pi}{2E}S_x S_\theta - \sum_{i=1}^{m}\sum_{j=1}^{n} t_{ij}^{S_x} \tag{A.7.4}$$

where

$$t_{ij}^{S_x} = \begin{cases} 0 & \text{i or j even} \\ f_{ij}^S \frac{S_x ta^3 L}{2E\pi ij}\left[\left(\frac{2j}{a}\right)^2 - \nu\left(\frac{\pi i}{L}\right)^2\right] & \text{else} \end{cases} \tag{A.7.5}$$

By differentiation, the stationary energy is:

$$\frac{\partial^2 T_{S_x}}{\partial a_{ij}\partial_{kl}} = -\frac{S_x taL\pi}{8}\left(\frac{\pi i}{L}\right)^2 \tag{A.7.6}$$

A.7.2 Potential energy due to stresses in the ring direction

The potential energy due to stresses in the ring direction is:

$$T_{S_\theta} = \int_0^L S_\theta t \triangle v(x) dx \tag{A.7.7}$$

where the elongation in the circumferential direction is:

$$\triangle v = \int_0^{\frac{\pi}{2}} \frac{v_{,\theta}}{a} a d\theta = \int_0^{\frac{\pi}{2}} \left(\varepsilon_\theta - \frac{w}{a} - \frac{w_{,\theta}^2}{2a^2}\right) d\theta \tag{A.7.8}$$

Using hooke's law and the stress function, the membrane strain can be written as:

$$\begin{aligned}\varepsilon_y =&\frac{1}{E}(-\nu\sigma_x + \sigma_y)\\ =&\frac{1}{E}\left(-\nu\left(-S_x - \sum_{i=1}^{m}\sum_{j_1}^{n} f_{ij}^{S}\sin\left(\frac{\pi i}{L}x\right)(2j)^2\sin(2j\theta)\right)\right.\\ &\left.+a^2\left(-\frac{S_\theta}{a^2} - \sum_{i=1}^{m}\sum_{j=1}^{n} f_{ij}^{S}\sin(2j\theta)\left(\frac{\pi i}{L}\right)\sin\left(\frac{\pi i}{L}x\right)\right)\right)\end{aligned} \tag{A.7.9}$$

Substituting the above relation into (A.7.9), using the assumed displacement function in Eq.(4.2.1) and integrating gives the potential energy due to circumferential stress:

$$T_{S_\theta} = -\sum_{i=1}^{m}\sum_{j=1}^{n}\frac{S_\theta t j^2 L\pi}{4a}a_{ij}a_{ij} - \frac{taL\pi}{2E}S_\theta^2 + \frac{\nu taL\pi}{2E}S_x S_\theta - \sum_{i=1}^{m}\sum_{j=1}^{n} t_{ij}^{S_\theta} \tag{A.7.10}$$

where

$$t_{ij}^{S_\theta} = \begin{cases} 0 & \text{i or j even}\\ f_{ij}^{S}\frac{S_\theta t a^3 L}{2E\pi ij}\left[\left(\frac{\pi i}{L}\right)^2 - \nu\left(\frac{2j}{a}\right)^2\right] & \text{else}\end{cases} \tag{A.7.11}$$

By differentiation, the stationary energy is:

$$\frac{\partial^2 T_{S_\theta}}{\partial a_{ij}\partial_{kl}} = -\frac{S_\theta t L\pi}{8a}(2j)^2 = -\frac{pL\pi}{8}(2j)^2 \tag{A.7.12}$$

A.7.3 Potential energy due to shear stresses

The potential energy due to shear stresses is:

$$\begin{aligned}T_{x\theta} &= \int_0^L\int_0^{\frac{\pi}{2}} S_{x\theta}t\left(\frac{u_{,\theta}}{a} + v_{,x}\right)ad\theta dx\\ &= \int_0^L\int_0^{\frac{\pi}{2}} S_{x\theta}t\left(\gamma_{x\theta} - w_{,x}\frac{w_{,\theta}}{a}\right)ad\theta dx\end{aligned} \tag{A.7.13}$$

Using hooke's law and the stress function, the membrane strain can be written as:

$$\begin{aligned}\gamma_{x\theta} &= \frac{2(1-\nu)}{E}\tau_{x\theta}\\ &= \frac{2a(1-\nu)}{E}\left(\frac{1}{a}S_{x\theta} - \sum_{i=1}^{m}\sum_{j=1}^{n} f_{ij}^{S}\left(\frac{\pi i}{L}\right)\cos\left(\frac{\pi i}{L}\right)(2j)\cos(2j\theta)\right)\end{aligned} \tag{A.7.14}$$

Substituting the above relation into (A.7.14), using the assumed displacement function in Eq.(4.2.1) and integrating gives the potential energy due to shear stresses:

$$T_{x\theta} = \frac{\pi a(1-\nu)tL}{E} S_{x\theta}^2 - \sum_{i=1}^{m}\sum_{j=1}^{n}\sum_{k=1}^{o}\sum_{l=1}^{p} \frac{S_{x\theta} t a_{ij} a_{kl} i l I_{ijkl}}{4} \tag{A.7.15}$$

where

$$I_{ijkl} = \begin{cases} 0 & \text{if i=k or j=l} \\ \left(\frac{\cos((l-j)\pi)-1}{l-j} - \frac{\cos((l+j)\pi)-1}{l+j}\right) * & \\ \left(\frac{\cos((k-i)\pi)-1}{k-i} - \frac{\cos((k+i)\pi)-1}{k+i}\right) & \text{else} \end{cases} \tag{A.7.16}$$

By differentiation, the stationary energy is:

$$\frac{\partial^2 T_{x\theta}}{\partial a_{ij} \partial a_{kl}} = -\frac{S_{x\theta} t i l}{4} I_{ijkl} \tag{A.7.17}$$

A.7.4 Potential energy due to external pressure

The potential due to external pressure is:

$$T_p = -\int_0^L \int_0^{\frac{\pi}{2}} p w d\theta dx \tag{A.7.18}$$

By substituting the assumed displacement field, and integrating, the result is:

$$T_p = \sum_{i=1}^{m}\sum_{j=1}^{n} \frac{apL}{2\pi ij} a_{ij} (\cos(\pi i) - 1)(\cos(\pi j) - 1) \tag{A.7.19}$$

Only terms of order $a_{ij}a_{kl}$ will make a contribution to the principle of stationary potential energy.

A.8 Rotational springs

A.8.1 Rotational spring at x=0

The strain energy for the rotational spring at $x = 0$:

$$U_{x=0}^S = \frac{1}{2} \int_0^{\frac{\pi}{2}} k_{x=0}^r (w_{ij,x} w_{kl,x})|_{x=0} \, a d\theta \tag{A.8.1}$$

Substituting the assumed displacement field, and integrating, gives the following result:

$$U^S_{x=0} = \sum_{ijk} \frac{\pi}{8} a k^r_{x=0} \left(\frac{\pi i}{L}\right) \left(\frac{\pi k}{L}\right) a_{ij} a_{kl}\ \delta_{j,l} \tag{A.8.2}$$

By differentiation, the stationary energy is:

$$\frac{\partial^2 U^S_{x=0}}{\partial a_{ij} \partial_{kl}} = \frac{a\pi^3 k^r_{x=0}}{4L^2} ik\ \delta_{q,s} \tag{A.8.3}$$

A.8.2 Rotational spring at x=L

The strain energy for the rotational spring at $x = L$:

$$U^S_{x=L} = \frac{1}{2} \int_0^{\frac{\pi}{2}} k^r_{x=L} (w_{ij,x} w_{kl,x})|_{x=L}\ a d\theta \tag{A.8.4}$$

Substituting the assumed displacement field, and integrating, gives the following result:

$$U^S_{x=L} = \sum_{ijk} \frac{\pi}{8} a k^r_{x=L} \left(\frac{\pi i}{L}\right) \left(\frac{\pi k}{L}\right) a_{ij} a_{kl} \cos(\pi i) \cos(\pi k)\ \delta_{j,l} \tag{A.8.5}$$

By differentiation, the stationary energy is:

$$\frac{\partial^2 U^S_{x=L}}{\partial a_{ij} \partial_{kl}} = \frac{a\pi^3 k^r_{x=L}}{4L^2} jl \cos(\pi i) \cos(\pi k)\ \delta_{q,s} \tag{A.8.6}$$

A.8.3 Rotational spring at θ=0

The strain energy for the rotational spring at $\theta = 0$:

$$U^S_{\theta=0} = \frac{1}{2} \int_0^L k^r_{\theta=0} (w_{ij,\theta} w_{kl,\theta})|_{\theta=0}\ dx \tag{A.8.7}$$

Substituting the assumed displacement field, and integrating, gives the following result:

$$U^S_{\theta=0} = \sum_{ijl} L k^r_{\theta=0} jl a_{ij} a_{kl}\ \delta_{i,k} \tag{A.8.8}$$

By differentiation, the stationary energy is:

$$\frac{\partial^2 U^S_{\theta=0}}{\partial a_{ij} \partial_{kl}} = 2L k^r_{\theta=0} qs\ \delta_{p,r} \tag{A.8.9}$$

A.8.4 Rotational spring at θ=$\pi/2$

The strain energy for the rotational spring at $\theta = \pi/2$:

$$U^S_{\theta=\frac{\pi}{2}} = \frac{1}{2}\int_0^L k^r_{\theta=\frac{\pi}{2}}(w_{ij,\theta}w_{kl,\theta})|_{\theta=\frac{\pi}{2}}\ dx \tag{A.8.10}$$

Substituting the assumed displacement field, and integrating, gives the following result:

$$U^S_\theta = \sum_{ijl} Lk^r_{\theta=\frac{\pi}{2}} a_{ij}a_{kl}\cos(\pi j)\cos(\pi l)\ \delta_{i,k} \tag{A.8.11}$$

By differentiation, the stationary energy is:

$$\frac{\partial^2 U^S_{\theta=\frac{\pi}{2}}}{\partial a_{ij}\partial_{kl}} = 2Lk^r_{\theta=\frac{\pi}{2}} qs\cos(\pi j)\cos(\pi l)\ \delta_{p,r} \tag{A.8.12}$$

Appendix B

Part of the Fortran code

B.1 Properties

```
PROGRAM Eigenproblem

    !Defines numeric precision
    USE kind_values,  only: wp => wp_swan

    REAL(wp) :: L, a, tp ,E, Ny, h, hr, ts, tsr, bf, tf, I_r, I_1, I_12, I_13,
     k_rot1, k_rot2,k_rot3, k_rot4, sig_x, pressure, tau_xy
    INTEGER iLambda, maxMs, maxNs , iNumDof
    !*****************************************************************************
    !* Shell properties                                                          *
    !*****************************************************************************
     L = 4200
     a = 1900
     tp = 14
     E = 206000
     Ny = 0.3
    !*****************************************************************************
    !* Stiffener Properties                                                      *
    !*****************************************************************************
     h = 300
     hr = 300
     ts = 15
     tsr = 15
     bf = 150
     tf = 20
    !*****************************************************************************
    !* Boundory conditions (Large stiffness = rigid supported)                   *
    !*****************************************************************************
     k_rot1 = 1000000
     k_rot2 = 1000000
     k_rot3 = 0000000
     k_rot4 = 0000000
    !*****************************************************************************
    !* Number of the eigenvalue                                                  *
    !*****************************************************************************
     iLambda = 1
    !*****************************************************************************
    !Degrees of freedom                                                         *
    !*****************************************************************************
     maxMs= 30
     maxNs= 30
     iNumDof = maxMs*maxNs
    !*****************************************************************************
    !* Load case                                                                 *
    !*****************************************************************************
     sig_x = 0
     tau_xy = 1
     pressure = 0
```

B.2 Eigenvalue

```
SUBROUTINE Eigenvalue(L, a, tp, E, Ny,  h, hr, ts, tsr, bf, tf, I_r, I_l, &
                      I_l2, I_l3, iLambda, iNumDof, maxMs, maxNs, &
                      k_rot1, k_rot2, k_rot3, k_rot4, sig_x, p, tau_xy)

    USE EigenproblemHandler
    USE kind_values,  only: wp => wp_swan    ! Defines numeric precision
    USE AVVIEWER

    IMPLICIT NONE

    REAL(wp) :: L, a, tp, E, C, Ny, y, h, hr, ts, tsr, bf, tf, I_r, I_l, I_l2, &
                I_l3, k, kTheta, D ,LAM, xValue, yValue, xArgument, yArgument, &
                sig_x, p, tau_xy, k_rot1, k_rot2, k_rot3, k_rot4, Int1shear, Int2shear , &
                Int3shear, Int4shear

    INTEGER iLambda, maxMs, maxNs , iNumDof

    INTEGER M, rowNr, columNr, intI, intJ, intK, intL, intM, intN, intO, intP, intQ, intR, &
            intS, number

    REAL,PARAMETER :: PI = 3.141592654

    REAL(wp), DIMENSION(iNumDof,iNumDof) :: KKBB, KKEIG

    REAL(wp), DIMENSION(iNumDof,iLambda) :: EigenVec
    REAL(wp), DIMENSION(iLambda) :: YMU


    REAL(wp), DIMENSION(50,50) :: w_r


     D   = (E*tp**3)/(12*(1-Ny**2))
     C   = (E*tp)/(1-ny**2)

     y   = (ts*h*h/2+bf*tf*(h+tf/2))/(ts*h+bf*tf)
     I_r = (tsr*hr**3)/12 + bf*tf**3/12 + tsr*hr*((hr/2+tp/2)**2) +bf*tf*((hr+tf/2+tp/2)**2)
     I_l = (ts*h**3)/12 + bf*tf**3/12  + ts*h*(h/2-y)**2 + bf*tf*(h+tf/2-y)**2  &
           +(ts*h+bf*tf)*(y+tp/2)**2
```

```
KKBB = 0
KKEIG = 0
w_r = 0

rowNr = 1

DO intI = 1, maxMs
    DO intJ = 1, maxNs

        columNr = 1

        !*****************************************************************************
        !* The diagonal contribution                                                 *
        !*****************************************************************************

        KKBB(rowNr,rowNr) = KKBB(rowNr,rowNr)  +PI*L*D*a/8 *((intI*PI/L)**2+(2*intJ/a)**2)**2 + &
                                PI/8*tp*L*E*(intI*PI/L)**4/(a*((intI*PI/L)**2+(2*intJ/a)**2)**2) !&
                                !- p*PI*intJ**2*L/2

        KKEIG(rowNr,rowNr) = KKEIG(rowNr,rowNr)  &!- p*PI*intJ**2*L/2 !&
                               - sig_x*tp*a*(intI**2)*(PI**3)/(8*L)

        !*****************************************************************************
        !*****************************************************************************

          DO intP = 1, maxMs
            DO intQ = 1, maxNs




        !*****************************************************************************
        !* Stringer stiffener contribution
        !*****************************************************************************


                IF(intI == intP) then
                KKBB(rowNr,columNr) = KKBB(rowNr,columNr) + E*I_l*PI**4/(2*L**3) &
                *intI**4 * sin(2*intJ*PI/4) *sin(2*intQ*PI/4)
                END IF


        !*****************************************************************************
        !*****************************************************************************


        !*****************************************************************************
        !* Ring stiffener contribution
        !*****************************************************************************


                IF(intJ == intQ) then
                KKBB(rowNr,columNr) = KKBB(rowNr,columNr) + E*I_r*PI/(a**3)  &
                *(1-(2*intJ)**2)**2 * (SIN(PI*intI/2)) * (SIN(PI*intP/2))
                END IF


        !*****************************************************************************
        !*****************************************************************************




!*****************************************************************************
!* Boundary conditions                                                       *
!*****************************************************************************
IF(intJ == intQ)Then
    !Boundary x=0
    KKBB(rowNr,columNr) = KKBB(rowNr,columNr) +  k_rot1 * intI*intP*a*PI*(PI/4*L)**2
    !Boundary x=L
    KKBB(rowNr,columNr) = KKBB(rowNr,columNr) +  k_rot2 * intI*intP*a*PI*(PI/4*L)**2 &
    * cos(intI*PI)*cos(intP*PI)
END IF
    IF(intI == intP)Then
    !Boundary theta=0
    KKBB(rowNr,columNr) = KKBB(rowNr,columNr) +  2 * k_rot3 * intJ*intQ*L/(a**2)
    !Boundary theta=Pi/2
    KKBB(rowNr,columNr) = KKBB(rowNr,columNr) +  2 * k_rot4 * intJ*intQ*L/(a**2) &
    * cos(intJ*PI)*cos(intQ*PI)
END IF
!*****************************************************************************
!*****************************************************************************
```

```
                !*************************************************************************
                !* Shear stress contribution                                             *
                !*************************************************************************
                Int1shear = (cos((intI+intP)*PI)-1)/(intI+intP)
                Int3shear = (cos((intJ+intQ)*PI)-1)/(intJ+intQ)
                IF(intI /= intP)Then
                    Int2shear = (cos((intP-intI)*PI)-1)/(intP-intI)
                ELSE
                    Int2shear = 0
                    Int1shear = 0
                END IF
                IF(intJ /= intQ)Then
                    Int4shear = (cos((intJ-intQ)*PI)-1)/(intJ-intQ)
                ELSE
                    Int4shear = 0
                    Int3shear = 0
                END IF
                KKEIG(rowNr,columNr) = KKEIG(rowNr,columNr) + tp*tau_xy/4*( intI*intQ* &
                (Int1shear+Int2shear)*(Int3shear+Int4shear) + intP*intJ*(Int1shear-Int2shear) &
                *(Int3shear-Int4shear) )
                !*************************************************************************
                !*************************************************************************

                columNr = columNr + 1
                END DO
            END DO
        rowNr = rowNr + 1
    END DO
END DO

!*****************************************************************************
!* Solving the eigenvalueproblem                                             *
!*****************************************************************************
CALL GiveInPutData(iLambda , 'M' , iNumDof, M , -KKEIG, KKBB)
CALL GetOutPutData( YMU , Eigenvec )
LAM = 1 / YMU(1)
!*****************************************************************************
!*****************************************************************************
```